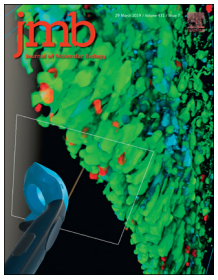

Evidence that Moderate Eviction of Spt5 and Promotion of Error-Free Transcriptional Bypass by Rad26 Facilitates Transcription Coupled Nucleotide Excision Repair

Kathiresan Selvam [1], Baojin Ding [2], Rahul Sharma [3] and Shisheng Li [1]

*1 - **Department of Comparative Biomedical Sciences,** School of Veterinary Medicine, Louisiana State University, Baton Rouge, LA 70803, USA*
*2 - **Department of Biology,** University of Louisiana at Lafayette, 410 E. St. Mary Blvd, Lafayette, LA 70503, USA*
*3 - **National Hansen's Disease Program,** Laboratory Research Branch at Louisiana State University, 3519E School of Veterinary Medicine, Baton Rouge, LA 70803, USA*

***Correspondence to Shisheng Li:** Department of Comparative Biomedical Sciences, School of Veterinary Medicine, Louisiana State University, Baton Rouge, LA 70803, USA. shli@lsu.edu*
https://doi.org/10.1016/j.jmb.2019.02.010
Edited by Kevin Struhl

Abstract

Transcription coupled repair (TC-NER) is a subpathway of nucleotide excision repair triggered by stalling of RNA polymerase at DNA lesions. It has been suspected that transcriptional misincorporations of certain nucleotides opposite lesions that result in irreversible transcription stalling might be important for TC-NER. However, the spectra of nucleotide misincorporations opposite UV photoproducts and how they are implicated in transcriptional stalling and TC-NER in the cell remain unknown. Rad26, a low abundant yeast protein, and its human homolog CSB have been proposed to facilitate TC-NER in part by positioning and stabilizing stalling of RNA polymerase II (RNAPII) at DNA lesions. Here, we found that substantial AMPs but no other nucleotides are transcriptionally misincoporated and extended opposite UV photoproducts and adjacent bases in *Saccharomyces cerevisiae*. Rad26 does not significantly affect either the misincorporation or extension of AMPs. At normally low or moderately increased levels, Rad26 promotes error-free transcriptional bypass and TC-NER of UV photoproducts. However, Rad26 completely loses these functions when it is overexpressed to ~1/3 the level of RNAPII molecules. Also, Rad26 does not directly displace RNAPII but constitutively evicts Spt5, a key transcription elongation factor and TC-NER repressor, from the chromatin. Our results indicate that transcriptional nucleotide misincorporation is not implicated in TC-NER, and moderate eviction of Spt5 and promotion of error-free transcriptional bypass of DNA lesions by Rad26 facilitates TC-NER.

Introduction

Nucleotide excision repair (NER) is a multistep process that removes bulky and/or helix-distorting DNA lesions, such as ultraviolet (UV)-induced dipyrimidine photoproducts, cyclobutane pyrimidine dimers (CPDs), and 6–4-photoproducts [1,2]. Transcription coupled NER (TC-NER) is a subpathway of NER that is dedicated to rapid removal of lesions in the transcribed strand of active genes [3–9]. Global genomic NER (GG-NER) is the other subpathway of NER that removes lesions throughout the genome [10]. The two NER subpathways differ only in the early lesion recognition steps but share the same NER factors in the later lesion verification, dual incision and excision, repair synthesis, and ligation steps [1,2].

In eukaryotic cell, TC-NER is believed to be triggered by stalling RNA polymerase II (RNAPII) [5,8,9]. UV photoproducts inhibit transcription elongation, and recovery of RNA synthesis occurs only after the lesions are repaired [11]. Bulky DNA lesions, such as CPDs and cisplatin adducts, have also been shown to efficiently stall RNAPII *in vitro* [12–14]. On a template containing a TT CPD, purified RNAPII incorporates AMP (A) opposite the 3′ T of the TT CPD [15–17]. However, primarily UMP (U) and, to a much lesser extent, A can be incorporated

opposite the 5′ T of the TT CPD. Incorporation of A opposite the 5′-T enables transcriptional bypass of the CPD, whereas misincorporation of U at this site results in irreversible stalling of RNAPII. It has therefore been proposed that misincorporation of nucleotide(s) that leads to transcription stalling may be important for TC-NER. To date, however, the spectra of nucleotide misincorporations opposite UV photoproducts and how they are implicated in transcriptional stalling and TC-NER in the cell remain unknown.

It has been well known that Rad26, a low-abundant DNA-dependent ATPase that is homologous to the human Cockayne syndrome B (CSB), plays an important role in TC-NER in *Saccharomyces cerevisiae* [18]. However, Rad26 is completely or partially dispensable for TC-NER in yeast cells lacking Rpb4 [19], Spt4 [20], certain domains of Spt5 (which is essential for cell viability) [21,22], and any subunit of the 5-subunit RNAPII associated factor complex (PAFc) [23]. Rpb4 is a non-essential subunit of RNAPII and forms a subcomplex with Rpb7, an essential subunit of RNAPII [24]. Spt4 and Spt5 are transcription elongation factors that form a complex [25]. It appears that the coordinated interactions of these factors with RNAPII hold the complex in a closed conformation that is highly competent for transcription elongation but intrinsically repressive to TC-NER [5]. Rad26 appears to facilitate TC-NER by antagonizing the repression. However, the underlying mechanism for the antagonization remains not well understood.

RNAPII has recently been shown to be dissociated from the chromatin after the step of dual incision of a transcription-blocking lesion [26]. However, how RNAPII behaves before the dual incision step that allows the trapped lesion to be recognized and repaired by the NER machinery has been enigmatic, although multiple models have been proposed [5,8,9]. Ubiquitination and degradation of Rpb1, the largest subunit of RNAPII [27,28], and TFIIS-facilitated backtracking of RNAPII [29,30] have been shown to play no role in TC-NER. *In vitro* studies have shown that both the yeast Rad26 [31] and human CSB [32] promote transcription elongation, facilitate transcriptional bypass of intrinsic pausing/arrest sequences, and resolve backtracking of RNAPII. However, neither Rad26 nor CSB is able to promote transcriptional bypass of a TT CPD *in vitro*. It has therefore been proposed that Rad26 and CSB might facilitate TC-NER in part by positioning and stabilizing stalling of RNAPII at lesion sites [31–33]. To date, however, no *in vivo* evidence has been available to support this proposition.

To gain insights into the TC-NER mechanisms, we performed high-resolution mappings of transcription across and TC-NER of UV photoproducts in yeast cells with well-controlled combinations of gene deletions and/or expressions. Here, we present evidence that transcriptional nucleotide misincorporation is not implicated in TC-NER, and moderate eviction of Spt5 and promotion of error-free transcriptional bypass of DNA lesions by Rad26 facilitates TC-NER.

Results

The ATPase activity of Rad26 is essential for its TC-NER function

Rad7 is essential for GG-NER but plays no role in TC-NER [2]. To specifically test the role of the ATPase activity of Rad26 in TC-NER, we transformed *rad7Δ rad26Δ* cells (Supplemental Table S1) with single-copy plasmids expressing the 3× FLAG-tagged wild-type (pRAD26) and helicase motifs Ia (pRAD26HIa), VI (pRAD26HVI) and Ia and VI (pRAD26HIa-VI) mutant Rad26 under the native *RAD26* gene promoter (Fig. 1a and Supplemental Table S2). The expression levels of the wild-type and helicase motif mutant Rad26 proteins were similar (Fig. 1b). To compare the level of the plasmid-expressed Rad26 to those of the endogenous Rad26 and RNAPII, we tagged the genomic *RAD26* and *RPB2* (encoding the second largest subunit of RNAPII) genes with 3× FLAG. It appeared that the level of the plasmid-expressed Rad26 was ~3/4 of that of the endogenously expressed Rad26 and ~1/350 of that of the Rpb2 in the cell (Fig. 1c). It has been previously estimated that about 90 and 30,000 molecules of Rad26 and RNAPII, respectively, are present in a yeast cell [34,35]. Our estimation of the ratio of Rad26 to RNAPII appears to be within the range of previous estimations.

The ATPase activities of the immunoprecipitated helicase motif mutant Rad26 were similar to that of mock immunoprecipitated samples (from *rad7Δ rad26Δ* cells containing the empty vector) (Fig. 1d), indicating that the mutant Rad26 proteins have no ATPase activity. The UV resistance of *rad7Δ rad26Δ* cells can be restored by pRAD26, but not by pRAD26HIa, pRAD26HVI, or pRAD26HIa-VI (Fig. 1e), indicating that the ATPase activity of Rad26 is essential for its TC-NER function. To confirm this notion, we directly measured TC-NER of CPDs. As expected, in *rad7Δ rad26Δ* cells containing an empty vector, repair of CPDs was defective in the transcribed strand of the *RPB2* gene, except for a short region of ~50 nucleotides (nt) immediately downstream of the transcription start site (from +1 to +50) (Fig. 2a). TC-NER in this short region has been known to be independent of Rad26 [19]. TC-NER was not restored upon complementation of the cells with pRAD26HIa, but was fully restored upon complementation with pRAD26 (Figs. 2a–c and 3a), indicating that the ATPase activity of Rad26 is indeed essential for its TC-NER function.

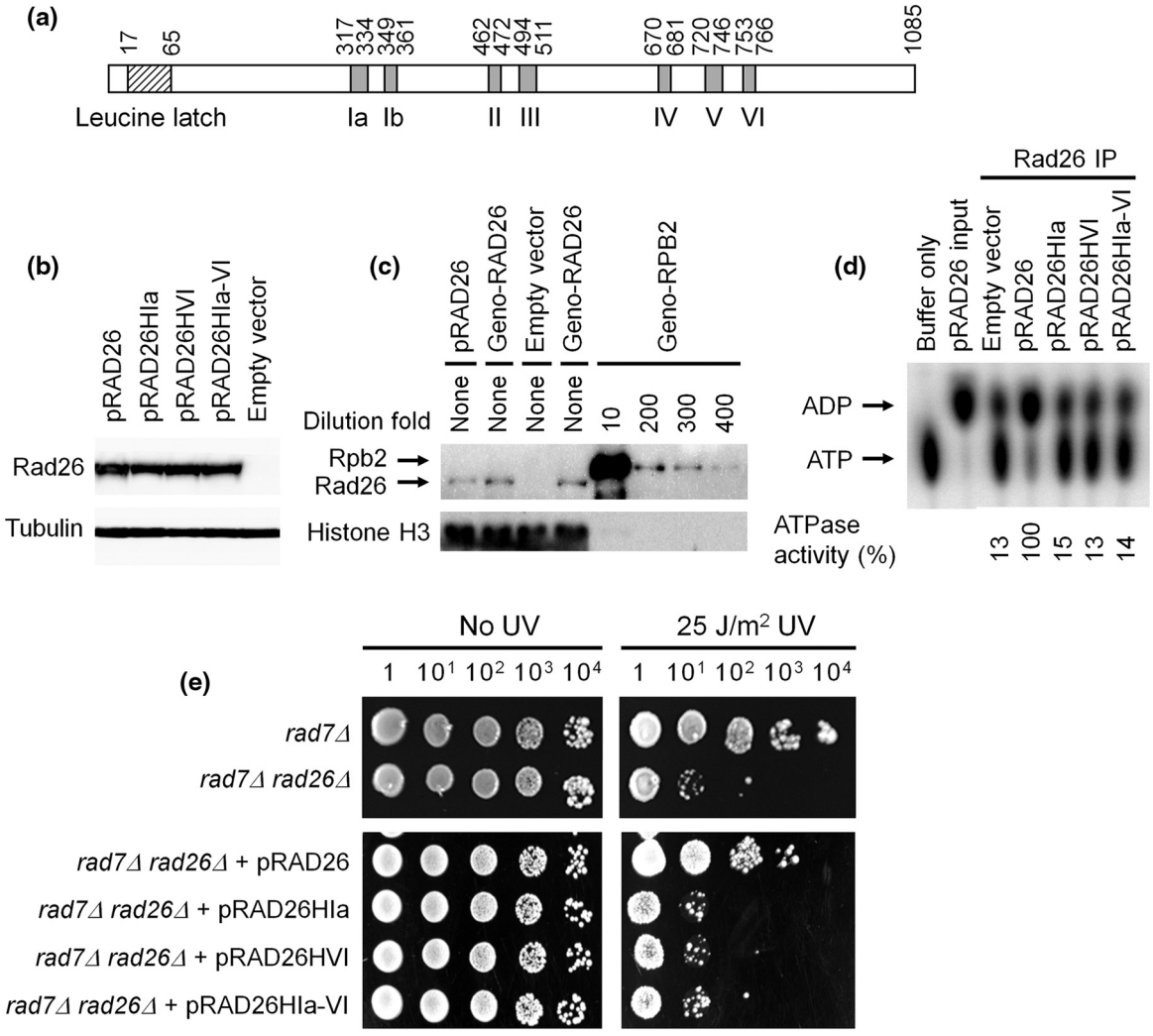

Fig. 1. Mutations of the helicase motifs Ia and/or VI of Rad26 inactivate the enzyme. (a) Schematic of the Rad26 protein. The leucine latch and seven canonical super family 2 helicase motifs are indicated. (b) Western blot showing the expression levels of 3× FLAG-tagged wild-type and helicase motif mutant Rad26 in *rad7Δ rad26Δ* cells containing the indicated plasmids. Tubulin serves as loading control. (c) Western blot showing levels of 3× FLAG-tagged Rad26 and Rpb2. Protein extracts were prepared from *rad7Δ rad26Δ* cells containing pRAD26 or the empty vector, and *rad7Δ* cells with genomic *RAD26* (Geno-RAD26) or *RPB2* (Geno-RPB2) gene tagged with 3× FLAG. As the level of Rpb2 is much higher than that of Rad26, the whole-cell protein extract for Rpb2 detection was diluted 10- to 400-fold before loading. Histone H3 serves as loading control. d) Developed TLC plates showing conversion of ATPs to ADPs by immunoprecipitated wild-type and helicase motif mutant Rad26. The ATPase activities (relative to the immunoprecipitated plasmid-expressed wild-type Rad26) were calculated by comparing the ADP/ATP ratios of the different samples. (e) UV sensitivity assay for the different strains. Saturated cultures were serially 10-fold diluted, spotted onto the plates, and irradiated with the indicated doses of 254 nm UV.

Only at normally low or moderately increased activities can Rad26 facilitate TC-NER

In vitro studies demonstrating the roles of the yeast Rad26 and human CSB in regulating transcription across a DNA lesion generally use high levels of these factors [31–33]. However, the cellular level of Rad26 is much lower than that of RNAPII (Fig. 1c). Also, different from its purified form, RNAPII is associated with a number of transcription elongation factors that repress TC-NER *in vivo* [5]. We therefore tested how TC-NER might be affected by different levels of Rad26 in the cell. We transformed *rad7Δ rad26Δ* cells with plasmids expressing Rad26 under its native promoter (pRAD26), the strong galactose-inducible *GAL10* promoter (pGAL-RAD26), or the moderately strong Cu^{2+}-inducible *CUP1* promoter (pCU-RAD26) (Supplemental Table S2). The ATPase activity of Rad26 is autoinhibited by the N-terminal leucine latch motif (Fig. 1a) and deletion or

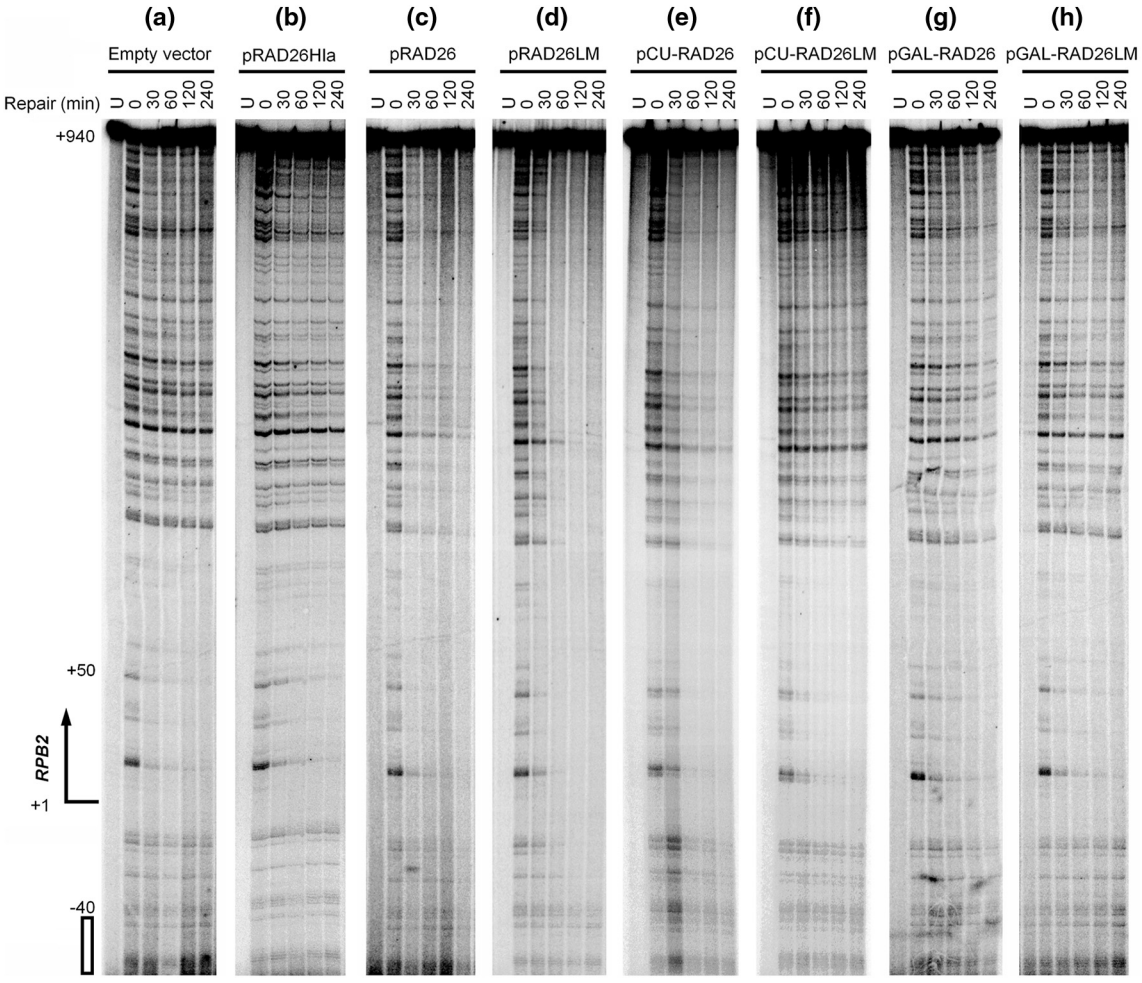

Fig. 2. TC-NER of CPDs in the transcribed strand of the *RPB2* gene. (a–h) sequencing gels showing CPDs remaining in galactose or $CuSO_4$-induced *rad7Δ rad26Δ* cells containing the indicated plasmids at different times of repair incubation. 'U' indicates samples from unirradiated cells. The top strong band corresponds to the full-length restriction fragment of the *RPB2* gene containing no DNA lesion. Bands below the top band correspond to CPD sites. Decrease of band intensities with time reflects repair. Approximate nucleotide positions relative to the transcription start site (+1) of the *RPB2* gene are indicated on the left of panel a. Open bar at the bottom left of panel A marks the upstream region (below –40) of the *RPB2* gene where only GG-NER but not TC-NER is operative and thus is not repaired in *rad7Δ* cells. The band intensities in this upstream region can be used to normalize signals in different lanes of the gels.

mutation of the leucine latch motif of Rhp26, the Schizosaccharomyces *pombe* homolog of the *S. cerevisiae* Rad26, has been shown to increase the ATPase activity ~4- to 5-fold [36]. To test the role of the leucine latch in TC-NER, we also transformed *rad7Δ rad26Δ* cells with plasmids expressing the leucine latch mutant Rad26 (Rad26LM) under its native promoter (pRAD26LM), the *GAL10* promoter (pGAL-RAD26LM), or the *CUP1* promoter (pCU-RAD26LM) (Supplemental Table S2). Rad26 and Rad26LM were expressed to similar levels under all the different promoters (Fig. 4a–c). After 4 h of galactose induction of the cells containing pGAL-RAD26 and pGAL-RAD26LM, the Rad26 and Rad26LM proteins reached the highest levels (Fig. 4b), which were ~120 times the normal expression level (Fig. 4d). At this high level of overexpression, the number of Rad26 or Rad26LM molecules would be ~1/3 of that of RNAPII molecules. Within 1 h of Cu^{2+} ($CuSO_4$) induction of the cells containing pCU-RAD26 and pCU-RAD26LM, the Rad26 or Rad26LM proteins reached the highest levels (Fig. 4c), which were ~20 times the normal expression level (Fig. 4d).

The *rad7Δ rad26Δ* cells containing pRAD26 and pRAD26LM showed similar TC-NER rates (Figs. 2c, d and 3a), indicating that, under the normally low expression level, the increased ATPase activity conferred by the leucine latch mutation does not dramatically affect TC-NER. The $CuSO_4$-induced cells containing pCU-RAD26 also showed normal TC-NER (Figs. 2e and 3a), indicating that a

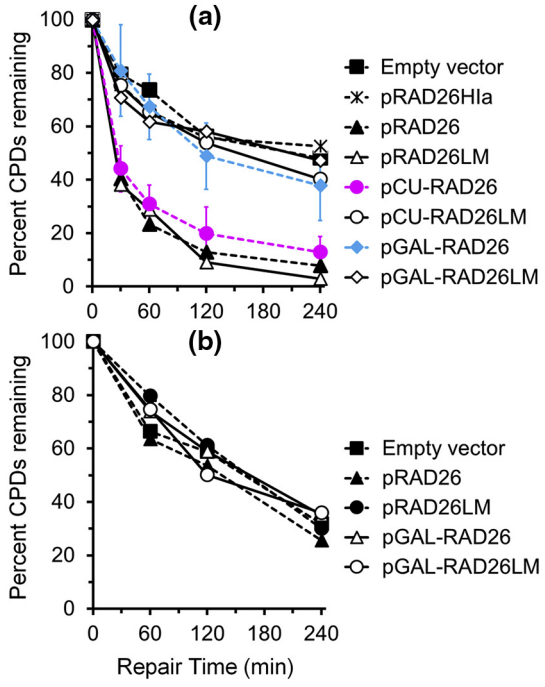

Fig. 3. CPDs remaining in the *RPB2* gene. (a) percent CPDs remaining in the transcribed strand (nt +60 to +900) of the *RPB2* gene in *rad7Δ rad26Δ* cells containing the indicated plasmids. CPDs located in the short region immediately downstream of the transcription start site were excluded for calculating the CPDs remaining, as TC-NER in this short region is independent of Rad26. Only the error bars (S.D.) for cells containing pCU-RAD26 (pink symbols) and pGAL-RAD26 (cyan symbols) are shown for clarity. (b) Percent CPDs remaining in the non-transcribed strand of the *RPB2* gene in *rad26Δ* cells containing the indicated plasmids.

moderate (~20 fold) overexpression of Rad26 did not significantly affect TC-NER. Surprisingly, the $CuSO_4$-induced cells containing pCU-RAD26LM showed a TC-NER rate that was similar to the cells containing an empty vector (Figs. 2a, f and 3a), indicating that the moderately overexpressed Rad26LM is not functional for TC-NER. The TC-NER rates in the galactose-induced cells containing pGAL-RAD26 or pGAL-RAD26LM were also similar to that in the cells containing an empty vector (Figs. 2a, g, h and 3a), indicating that the highly (~120 fold) overexpressed Rad26 or RAD26LM is not functional for TC-NER. Taken together, our results indicate that at a high level of activity, achieved by overexpressing either Rad26 to ~1/3 or Rad26LM to ~1/17 the level of RNAPII molecules, Rad26 loses its function for TC-NER. Taking into the consideration that the ATPase activity of Rad26LM is ~4–5 times that of the wild-type Rad26, we estimate that Rad26 loses its function for TC-NER when its activity is increased to ~100 times that of its normal level.

The rates of CPD removal in the non-transcribed strand of the *RPB2* gene appeared to be similar in cells expressing the different levels of Rad26 or Rad26LM (Fig. 3b and Supplemental Fig. S1), indicating that the increased Rad26 activities did not significantly affect GG-NER.

Only at normally low or moderately increased activities can Rad26 efficiently promote transcriptional bypass of UV photoproducts

Based on *in vitro* studies, it has been proposed that Rad26 and its human homolog CSB might facilitate TC-NER in part by positioning and stabilizing stalling of RNAPII at lesion sites [31–33]. To determine if the modulation of TC-NER by the different activities of Rad26 was achieved by modulating transcription stalling at UV photoproducts, we fine-mapped transcription on a UV damaged template in the cell. To avoid interference by preexisting RNAs, we analyzed galactose-induced transcripts of the genomic *GAL10* gene, which has undetectable leakage transcription in the absence of galactose [37]. Like its human homolog XPA, Rad14 plays an important role in lesion recognition/verification and is essential for both TC-NER and GG-NER [2]. Elc1 is a component of a ubiquitin ligase complex that is required for ubiquitination and degradation of RNAPII upon DNA damage [38] but plays no role in TC-NER [27]. To prevent repair of UV photoproducts and degradation of RNAPII during the transcription analyses (which would skew the transcription results), we used *rad7Δ rad26Δ rad14Δ elc1Δ* cells (Supplemental Table S1) containing an empty vector, pRAD26, pCU-RAD26, or pCU-RAD26LM (Supplemental Table S2). The cells were induced with $CuSO_4$ to moderately overexpress Rad26 (which enables the TC-NER function) or Rad26LM (which disables the TC-NER function) in cells containing pCU-RAD26 or pCU-RAD26LM, UV irradiated (240 J/m^2) to produce ~1 CPDs/kb of single-stranded DNA and switched to galactose medium to induce transcription of the *GAL10* gene.

Full-length and nascent *GAL10* transcripts became detectable in all unirradiated cells shortly after galactose induction (Supplemental Fig. S2). However, mostly nascent and only a little full-length *GAL10* transcripts could be detected in the UV-irradiated cells (Supplemental Fig. S2), indicating stalling of transcription by UV photoproducts.

We then sequenced the nascent *GAL10* transcripts that were ≤800 nt long (Fig. 5). To exclude sequencing artifacts, the transcripts were ligated to an single-stranded DNA adapter that contains a region of random nucleotides, which serves as a Unique Molecular Identifier (UMI) so that PCR duplicates and sequencing errors (which are typically 0.1$–1% for next-generation sequencing) can be removed/corrected [39] (Fig. 5c). Equal amounts of barcoded sequencing libraries prepared from different cell samples were combined, and the

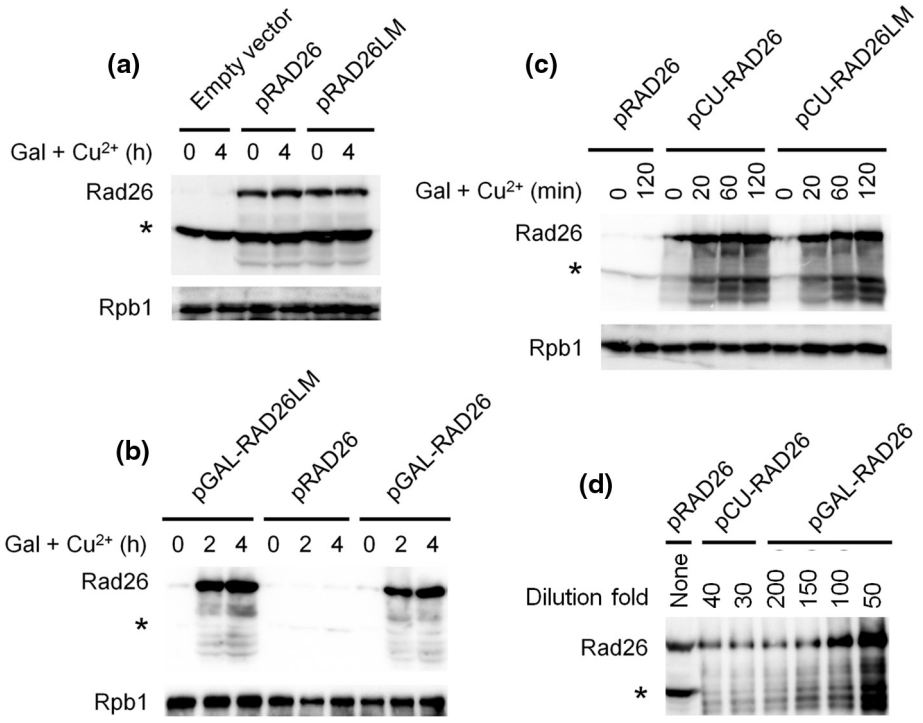

Fig. 4. Levels of expressions of Rad26 and Rad26LM. (a–c) Western blots showing levels of Rad26 and Rad26LM in *rad7Δ rad26Δ* cells containing the indicated plasmids at different times after additions of galactose and $CuSO_4$. (d) Western blot showing levels of Rad26 and Rad26LM after dilutions of the protein extracts. The protein extracts diluted were prepared from cells containing pGAL-RAD26 after 4-h galactose induction and from cells containing pCU-RAD26 after 1 h of $CuSO_4$ induction. The asterisk indicates a non-specific band. Rpb1 serves as loading control.

fragments with the insert sizes of ≤800 nt were gel purified and sequenced. The length distributions of the nascent *GAL10* transcripts were similar among the unirradiated cells containing the different plasmids (Fig. 6a, d, g, and j). At 20 min of galactose induction, the length distribution was somewhat more toward the longer transcripts in the UV-irradiated cells containing pRAD26 or pCU-RAD26 than those containing the empty vector or pCU-RAD26LM (Fig. 6b, e, h, and k). At 40 min of galactose induction, the length distribution shifted more toward the longer transcripts in the UV-irradiated cells containing pRAD26 (Fig. 6, compare e and f) or pCU-RAD26 ((Fig. 6, compare h and i). Indeed, in the cells containing pRAD26 or pCU-RAD26, the $\log_2$ ratios of the numbers of longer (>250 nt) transcripts at 40 min to those at 20 min of galactose induction were generally >0 (indicating increase of the numbers of longer transcripts), whereas the $\log_2$ ratio of the numbers of shorter (< 250 nt) transcripts was generally <0 (indicating decrease of the numbers of shorter transcripts) (Fig. 6n and o). However, the length distribution did not change significantly with time in the cells containing either the empty vector (Fig. 6b, c, and m) or pCU-RAD26LM (Fig. 6k, l, and p). These results indicate that, only at normally low or moderately increased activities, can Rad26 promote transcriptional bypass of UV lesions in the cell.

UV photoproducts occur at di-pyrimidine sites with the frequencies in the order of (3′ → 5′) TT > TC = CT > CC [40]. We analyzed transcripts ended opposite the di-pyrimidine sites and flanking sequences within the first 550-nt region of the transcribed strand of the *GAL10* gene. Transcription may also stall at certain intrinsic pausing sites. However, the intrinsic stalling is generally transient, as evidenced by the fact that within 5 min of induction, full-length *GAL10* mRNA can be detected in unirradiated cells (Supplemental Fig. S2). Also, once *GAL10* transcription is fully induced, the distribution of nascent transcripts ended at different sites along the *GAL10* genes will not change in unirradiated cells (although the total transcripts will increase with time until a steady state is reached). Therefore, by comparing the counts of nascent *GAL10* transcripts ended opposite the di-pyrimidine sites and flanking sequences between UV-irradiated and -unirradiated samples, we will be able to assess how transcription may be stalled by UV photoproducts. At 20 min of galactose induction, the nascent *GAL10* transcripts ended opposite the purines 3′ to

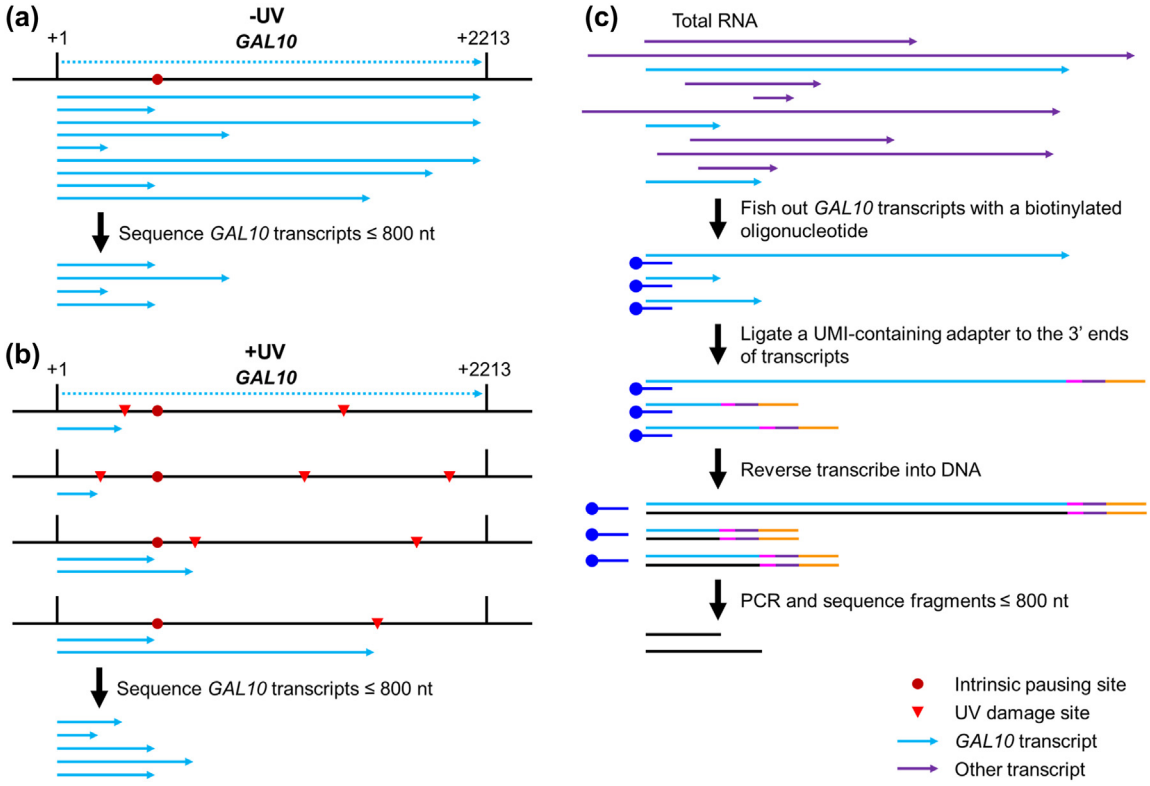

Fig. 5. Outline for analyses of *GAL10* transcripts in UV-irradiated and -unirradiated NER-deficient (*rad14Δ*) cells. (a and b) Schematics showing *GAL10* transcripts that may stall at UV damage and/or intrinsic pausing sites. (c) outline for creating a next-generation sequencing library of *GAL10* transcripts. Note that only transcripts ≤800 nt would be sequenced for analyses.

the di-pyrimidine sites (A/G – 1) were significantly higher in all the UV-irradiated cells than in the unirradiated ones (Fig. 7a, c, e, and g), indicating stalling of transcription by the UV photoproducts. Significant transcription stalling could also be seen opposite the 3′ C (C1) in CT (Fig. 7c), and the 3′ T (T1) in TT (Fig. 7g). At 40 min of galactose induction, stalling of the *GAL10* transcription opposite the A/G – 1, C1, and T1 persisted (the $\log_2$ ratios did not significantly change) in UV-irradiated cells containing the empty vector or pCU-RAD26LM but disappeared (the $\log_2$ ratios decreased to near 0) in those containing pRAD26 or pCU-RAD26 (Fig. 7b, d, f, and h). These results, together with our above observations (Fig. 6), indicate that only at normally low or moderately increased activities can Rad26 promote transcriptional bypass of UV photoproducts in the cell. These findings are surprising because neither Rad26 [31] nor CSB [32] is able to promote transcriptional bypass of a TT CPD *in vitro*. Also, while the positioning and stabilization of RNAPII at lesions by Rad26 and CSB may be important for initial lesion detection [31,32], our results indicate that the function for promoting transcriptional bypass of DNA lesions is required for Rad26 to facilitate TC-NER.

Only AMPs are substantially misincorporated and extended opposite UV photoproducts and adjacent bases; Rad26 does not significantly affect either misincorporation or extension of AMPs but at normally low or moderately increased activities promotes error-free transcriptional bypass of UV photoproducts

Previous *in vitro* studies have shown that U misincorporation opposite the 5′ T of a TT CPD results in irreversible stalling of RNAPII, which was suspected to be important for elicitation of TC-NER [15,16]. To determine if incorporation or misincorporation of specific nucleotides is required for transcriptional stalling at UV photoproducts and TC-NER in the cell, we analyzed the nucleotides at the 3′ ends of nascent *GAL10* transcripts. Significant misincorporations of AMPs (As) could be seen at the 3′ ends of the nascent transcripts opposite A/G – 1 3′ to all dipyrimidine sites, C1 in CC and CT, and A/G + 1 5′ to TT in all the UV-irradiated cells containing

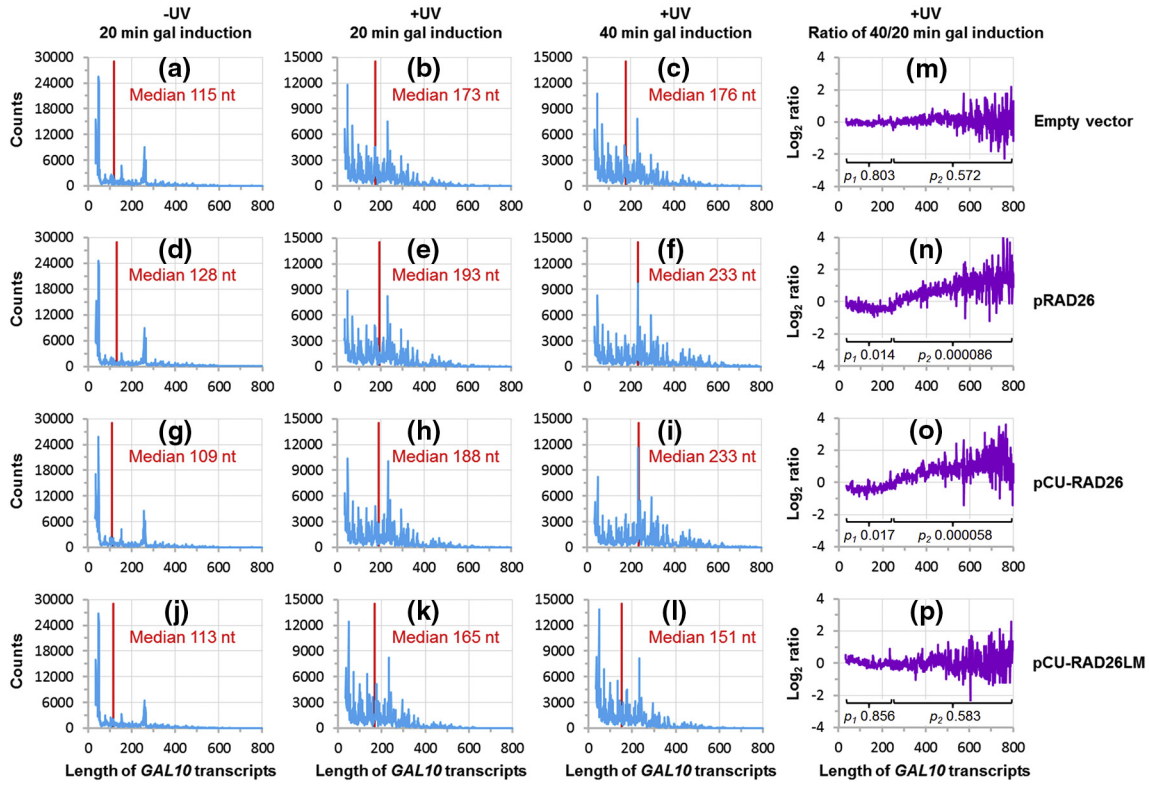

Fig. 6. Length distributions of nascent *GAL10* transcripts. (a–l) Plots showing length distributions of sequenced nascent *GAL10* transcripts. Cyan lines indicate counts of transcripts of different lengths (in nts) (normalized to 5×10^5 total reads for each sample). The red bar in each of the panels indicates the median length of transcripts. (m–p) Log_2 ratio of corresponding transcript counts shown in panels c and b, f and e, i and h, and l and k, respectively. p_1 shown in panels m, n, o, and p is the *p* value of two-tailed Student's *t* test of the counts of short transcripts (34–249 nt) between the respective + UV samples of 40 and 20 min of galactose induction. p_2 shown in panels m, n, o, and p is the *p* value of two-tailed Student's *t* test of the counts of longer transcripts (251–800 nt) between the respective + UV samples of 40 and 20 min of galactose induction. Plasmids contained in the *rad7Δ rad26Δ rad14Δ elc1Δ* cells are indicated on the right.

the different plasmids (Fig. 8, pink symbols). Also, significant AA misincorporations were seen at the 3′ ends of the nascent transcripts opposite C2 in CC (the 5′ A opposites C1 and the 3′ A opposites C2), T2 in CT (the 5′ A opposites C1 and the 3′ A opposites T2), T1 in TT (the 5′ A opposites A/G – 1 and the 3′ A opposites T1), and N + 2 5′ to TT (the 5′ A opposites A/G + 1 and the 3′ A opposites N + 2) in all the UV-irradiated cells containing the different plasmids (Fig. 8, cyan symbols). No significant misincorporation of other nucleotides could be seen at the 3′ ends of the nascent transcripts, including misincorporations of Us opposite the 5′ T of TT as seen by previous *in vitro* studies [15–17]. The A or AA misincorporations appeared similar in the cells containing the different plasmids, indicating that the different Rad26 activities did not significantly affect A or AA misincorporations.

To understand if transcriptional bypass of UV photoproducts involves misincorporations of certain nucleotides, we analyzed misincorporated nucleotides in the internal regions (i.e., not at the ends) of the nascent *GAL10* transcripts. At 20 min of galactose induction, significant misincorporations of As could be seen opposite A/G – 1 3′ to all dipyrimidine sites, C1 in CC and CT and A/G + 1 5′ to TT in all the UV-irradiated cells containing the different plasmids (Fig. 9a, c, e, and g, pink symbols). At 40 min of galactose induction, the frequencies of A misincorporations were somewhat lower opposite certain sites (not always statistically significant) in cells containing pRAD26 and pCU-RAD26 than those containing the empty vector or pCU-RAD26LM (Fig. 9b, d, f, and h). Misincorporations of other nucleotides were rare and not significantly different between UV-irradiated and -unirradiated cells (Fig. 9). These results indicate that UV photoproducts can be transcriptionally bypassed following misincorporations of As regardless of Rad26 activities. Taken together, our results also indicate that Rad26, at normally low or moderately increased activities, primarily promotes error-free transcriptional bypass of UV photoproducts.

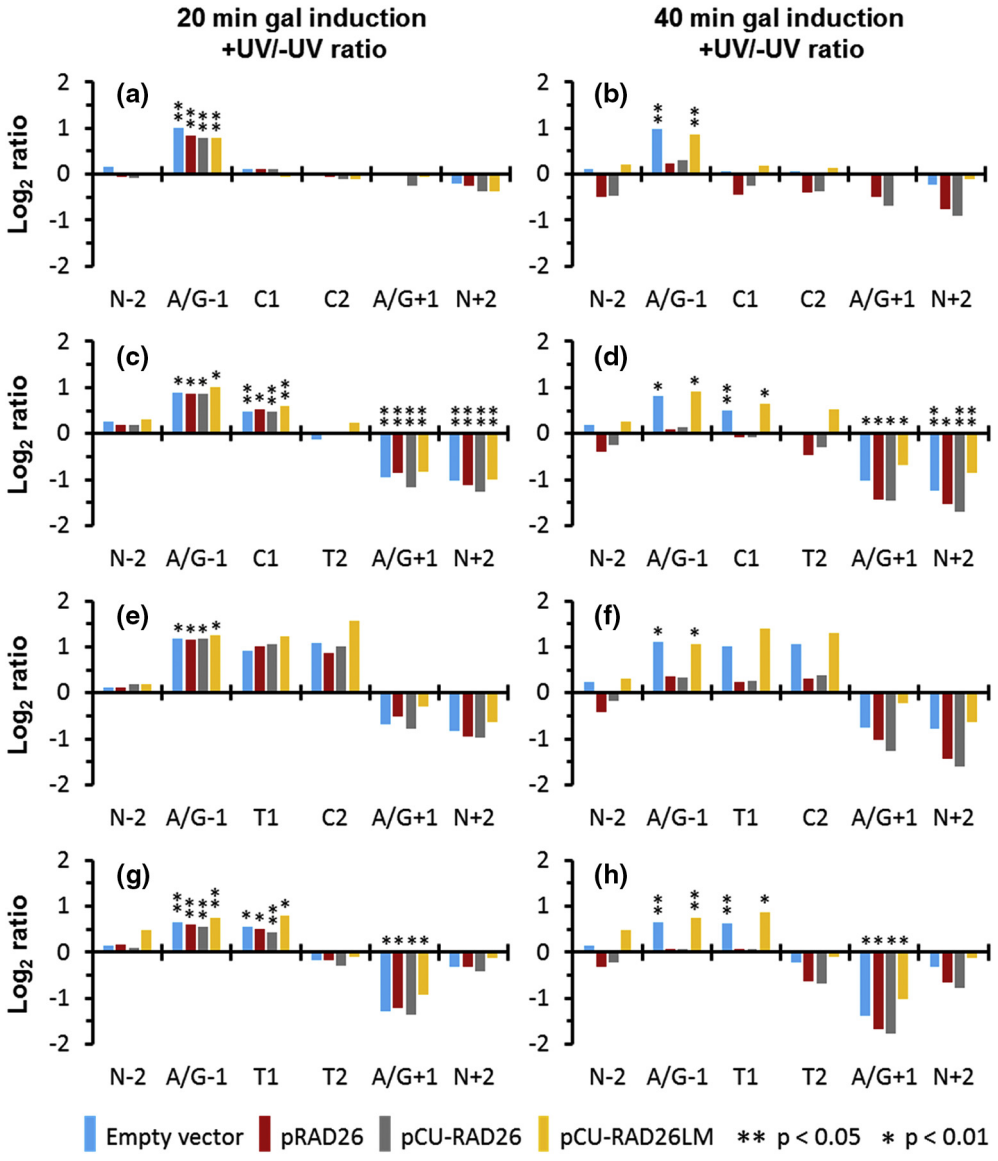

Fig. 7. Transcription stalling opposite UV photoproducts and flanking sequences. (a–h) Log_2 ratio (+UV/−UV) of counts of nascent *GAL10* transcripts ended opposite CC (a and b), CT (c and d), TC (e and f), TT (g and h), and flanking sequences. Plasmids contained in the *rad7Δ rad26Δ rad14Δ elc1Δ* cells are shown in different colors as indicated at the bottom. A/G − 1 and A/G + 1 are purines immediately 3′ and 5′ to the di-pyrimidine sites, respectively. N − 2 and N + 2 are the second nucleotide 3′ and 5′ to the di-pyrimidine site, respectively, and are neither within nor neighbored by di-pyrimidine sites. The normalized counts from the UV-irradiated cells were divided by the corresponding ones from the unirradiated cells. Bars represent the means of log_2 count ratios of all transcripts (with or without nucleotide misincorporation at the 3′ ends) ended opposite all the relevant positions within the first 550-nt region of the transcribed strand of the *GAL10* gene. Single and double asterisks indicate that the counts are significantly different between UV-irradiated and -unirradiated cells (p values <0.01 and 0.05, respectively; paired and two-tailed Student's t test).

The inability of a high level of Rad26 activity to facilitate transcriptional bypass of UV photoproducts is not due to displacement of RNAPII

Why a high level of Rad26 activity, like in the absence of Rad26, is unable to facilitate transcriptional bypass of DNA lesions and TC-NER? Under physiological conditions, the RNAPII complex stalled at a lesion is extremely stable [41]. We wondered if a high level of Rad26 activity could displace RNAPII from the UV damaged template, thereby disabling transcriptional bypass of DNA lesions and TC-NER. We compared the levels of Rpb1, the largest subunit of RNAPII, in the chromatin and non-chromatin

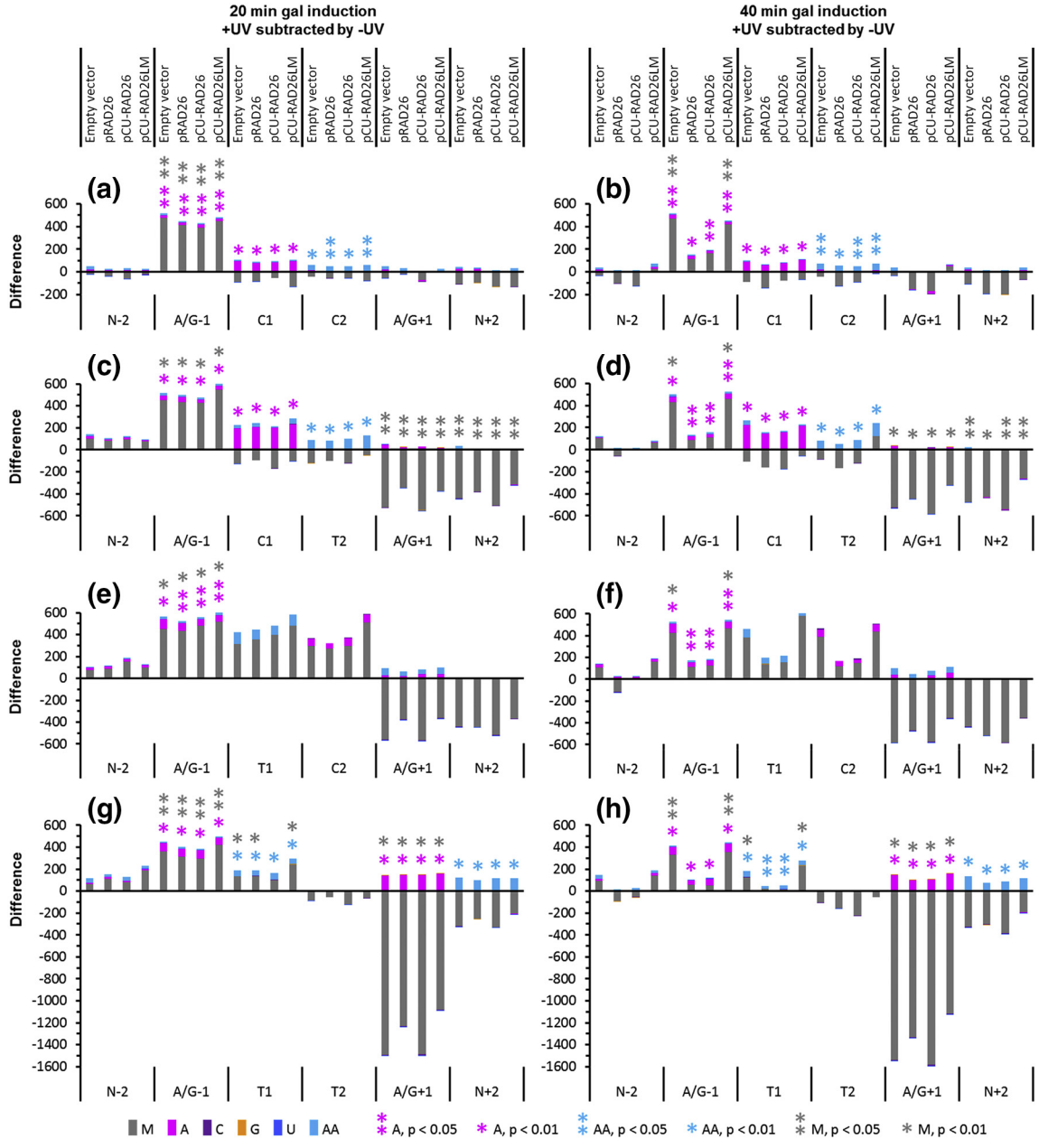

Fig. 8. Nucleotides at the 3′ ends of nascent *GAL10* transcripts opposite UV photoproducts and flanking sequences. (a–h) Count differences (between + UV and – UV) of nucleotides at the 3′ ends of nascent *GAL10* transcripts opposite CC (a and b), CT (c and d), TC (e and f), TT (g and h), and flanking sequences. Plasmids contained in the *rad7Δ rad26Δ rad14Δ elc1Δ* cells are indicated at the top. A/G – 1 and A/G + 1 are purines immediately 3′ and 5′ to the di-pyrimidine sites, respectively. N – 2 and N + 2 are the second nucleotide 3′ and 5′ to the di-pyrimidine site, respectively, and are neither within nor neighbored by di-pyrimidine sites. The counts of transcripts with matched (M, gray bars) or misincorporated nucleotides (A, C, G, U, or AA, shown in different colors as indicated at the bottom) at the 3′ ends were normalized to 10^5 total reads across the nucleotide positions (which include all reads that are the same length or longer than the transcripts). The counts from the UV-irradiated cells were subtracted by the corresponding ones from the unirradiated cells. Bars represent the means of count differences of the 3′ end nucleotides opposite all the relevant positions within the first 550-nt region of the transcribed strand of the *GAL10* gene. Single and double asterisks with colors matching those of the 3′ end nucleotides indicate that the counts are significantly different between UV-irradiated and -unirradiated cells (*p* values <0.01 and 0.05, respectively; paired and two-tailed Student's *t* test).

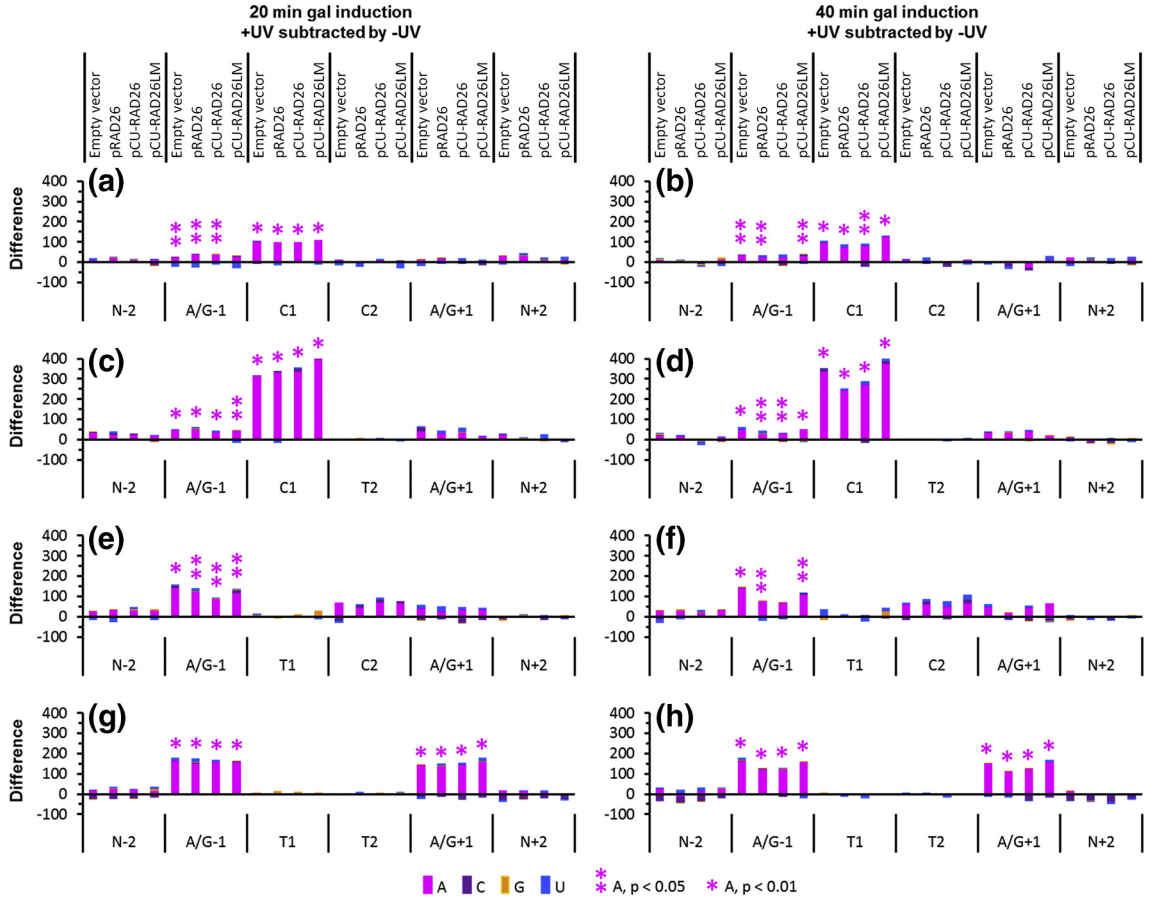

Fig. 9. Nucleotide misincorporations in the internal region of nascent *GAL10* transcripts opposite UV photoproducts and flanking sequences. (a–h) Count differences (between +UV and −UV) of misincorporated nucleotides in the internal regions of nascent *GAL10* transcripts opposite CC (a and b), CT (c and d), TC (e and f), TT (g and h), and flanking sequences. Plasmids contained in the *rad7Δ rad26Δ rad14Δ elc1Δ* cells are indicated at the top. A/G – 1 and A/G + 1 are purines immediately 3′ and 5′ to the di-pyrimidine sites, respectively. N – 2 and N + 2 are the second nucleotide 3′ and 5′ to the di-pyrimidine site, respectively, and are neither within nor neighbored by di-pyrimidine sites. The counts of misincorporated nucleotides (A, C, G, U, shown in different colors as indicated at the bottom) were normalized to 10^5 total reads across the respective nucleotide positions (which include all reads that are the same length or longer than the transcripts). The counts from the UV-irradiated cells were subtracted by the corresponding ones from the unirradiated cells. Bars represent the means of count differences of the misincorporated nucleotides opposite all the relevant positions within the first 550-nt region of the transcribed strand of the *GAL10* gene. Pink single and double asterisks indicate that the counts of misincorporated As are significantly different between UV-irradiated and -unirradiated cells (p values <0.01 and 0.05, respectively; paired and two-tailed Student's t test).

fractions in galactose-induced *rad7Δ rad26Δ rad14Δ elc1Δ* cells containing an empty vector with those containing pGAL-RAD26LM (Supplemental Fig. S3). As expected, histone H3 was primarily present in the chromatin fraction, whereas the cytoplasmic protein GAPDH was primarily present in the supernatant (Supplemental Fig. S3B). The levels of Rpb1 in chromatin and supernatant fractions in the UV-irradiated cells containing pGAL-RAD26LM were similar to those in the cells containing the empty vector, and the levels did not change significantly with time (Supplemental Fig. S3C and D). These results indicate that the inability of a high level of Rad26 activity to facilitate transcriptional bypass of UV photoproducts and TC-NER is not due to displacement of RNAPII from the template.

Rad26 evicts Spt5 from chromatin

Rad26 has recently been shown to bind to the clamp and stalk (Rpb4/7) regions of RNAPII *in vitro* [31]. These binding sites on RNAPII partially overlap with those of Spt5 [22,31], a key transcription elongation factor that coordinates the repression of TC-NER [5]. Rad26 may modulate TC-NER by affecting the interaction of Spt5 with RNAPII in the cell. To test this possibility, we compared the levels of Spt5 in the chromatin and non-chromatin fractions

in *rad7Δ rad26Δ rad14Δ elc1Δ* cells containing an empty vector or those expressing different levels of Rad26 or Rad26LM. Indeed, the levels of Spt5 associated with chromatin were inversely correlated with the levels of Rad26 activity, and UV irradiation did not significantly affect the chromatin association (Fig. 10a and b). This is in line with the previous report showing that Rad26 is recruited to the coding sequences of genes in a transcription-dependent but DNA-lesion-independent manner [42]. Our results indicate that Rad26 constitutively evicts Spt5 from chromatin and the degree of the eviction is correlated with the activities of Rad26.

Discussion

We, for the first time, analyzed the spectra of nucleotides transcriptionally incorporated opposite UV photoproducts and how they are implicated in transcriptional stalling, bypass, and TC-NER in the cell. We found that only As but no other nucleotides are significantly misincorporated into transcripts and extended opposite both the 3′ and 5′ bases in a UV photoproducts. We also observed significant A misincorporations and extensions opposite the bases immediately 3′ to all pyrimidine dimers and 5′ to TTs. These findings suggest that nucleotide misincorporations and extensions by RNAPII opposite UV photoproducts and adjacent bases in the cell follow the A-rule as commonly known for error-prone DNA polymerases [43]. Furthermore, we found that different Rad26 activities do not significantly affect

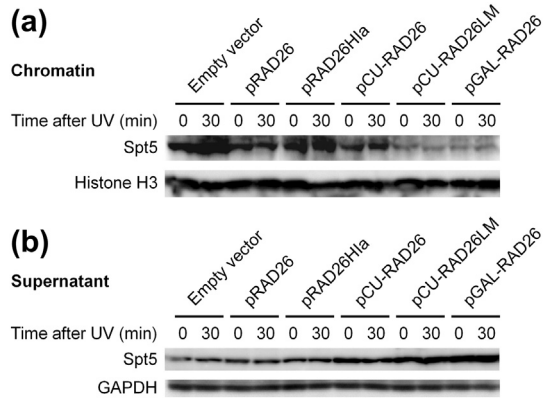

Fig. 10. Rad26 weaken the association of Spt5 with chromatin. (a and b) Western blots showing the levels of Spt5 presented in the chromatin (a) and supernatant (b), respectively, in cells at 0 or 30 min after UV irradiation. Prior to UV irradiation, the cells containing pGAL-RAD26 were induced with galactose for 4 h and those containing pCU-RAD26 and pCU-RAD26LM were induced with $CuSO_4$ for 1 h. Following UV irradiation, the cells were incubated in the same respective inducing media. Histone H3 and GAPDH serve as loading controls for chromatin and supernatant fractions, respectively.

either misincorporation or extension of As. Taken together, our results indicate that promotion of TC-NER of UV photoproducts by Rad26 does not require nucleotide misincorporations that result in irreversible transcriptional stalling.

In vitro studies have demonstrated that Rad26 [31] and CSB [32] are able to resolve backtracking of RNAPII but cannot enable transcriptional bypass of a TT CPDs. We found that, at moderate activities but not at high activities, Rad26 promotes transcriptional bypass of UV photoproducts *in vivo*. It is possible that the levels of Rad26 and CSB used by the *in vitro* studies are too high to allow for transcriptional bypass of the UV photoproduct. RNAPII is associated with multiple transcription elongation factors. It is also possible that transcriptional bypass of UV photoproducts may require the participation of these transcription elongation factors after being remodeled by moderate activities of Rad26.

Rad26 has recently been shown *in vitro* to bind to the DNA upstream of the RNAPII elongation complex and sits between the RNAPII clamp and stalk (Rpb4/7) regions [31]. These binding sites on RNAPII overlap with those of Spt5 [22,31]. Based the previous reports and our findings here, we propose the following model for how Rad26 facilitates TC-NER. In the absence of Rad26, a DNA lesion is trapped in the RNAPII complex, which is stabilized by coordinated actions of Spt5 and other transcription elongation factors, and TC-NER is repressed (Fig. 11a). At normally low or moderately increased activities, Rad26 may transiently bind to and "loosen" the RNAPII complex by competing with Spt5, which enables trans-lesion transcription leading to exposure, dual incision, and excision of DNA lesions behind the RNAPII complex (Fig. 11b). The excised fragment containing the DNA lesion may dissociate from the chromatin along with RNAPII as shown in human cells [26]. However, RNAPII does not dissociate from the chromatin if TC-NER does not proceed past the dual incision step (e.g., in NER-defective *rad14Δ* cells). In view of the fact that TC-NER is very rapid, whereas the Rad26-mediated trans-lesion transcription appears to be fairly slow in the absence of NER (in *rad14Δ* cells), it is likely that TC-NER may be able to initiate at an early stage of the trans-lesion transcription. It is also possible that Rad26 promotes trans-lesion synthesis more rapidly in the presence of the NER machinery. At a high level of activity, achieved by overexpressing the Rad26 or Rad26LM to ~1/3 or 1/17 the level of RNAPII molecules, respectively, Rad26 may severely disrupt the binding of Spt5 (and other transcription elongation factors) to RNAPII, resulting in impairments of trans-lesion transcription and repression of TC-NER (Fig. 11c). It is quite unlikely that the overexpression of Rad26, especially that driven by the *GAL10* promoter, will cause dramatic Rad26 misfolding because the overexpressed

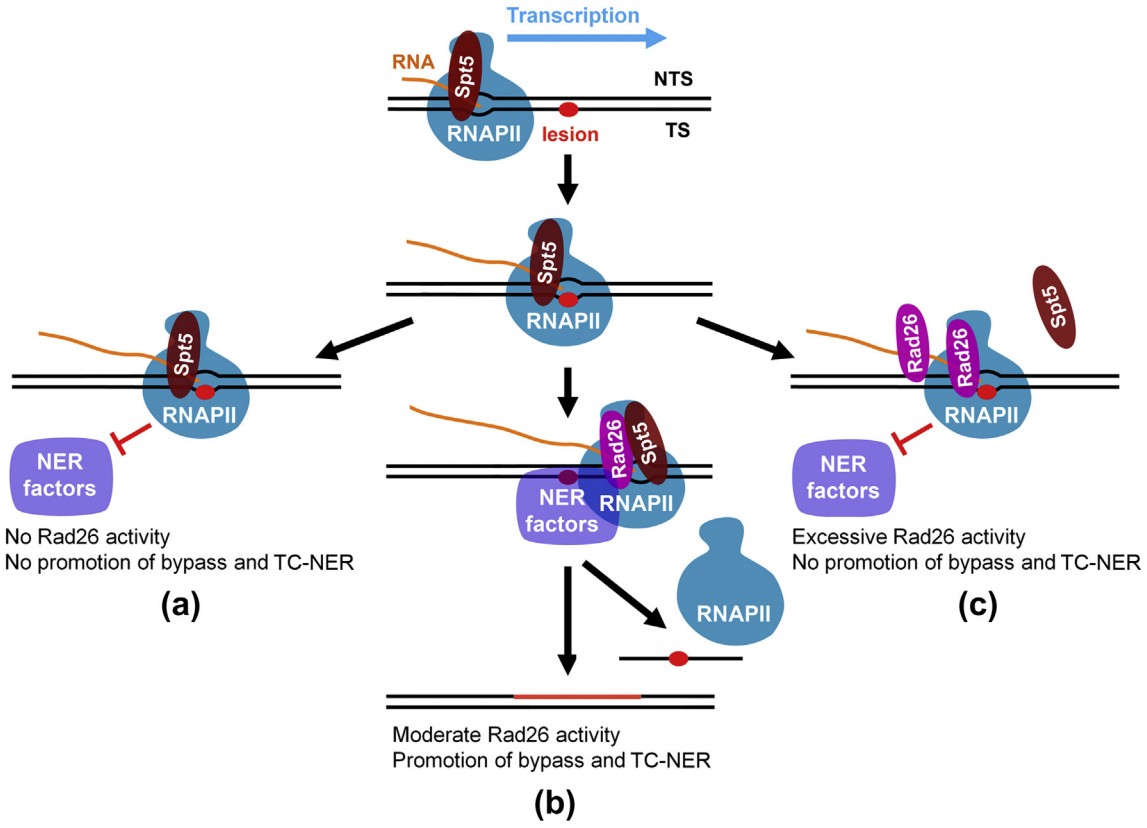

Fig. 11. Proposed mechanism of how Rad26 facilitates TC-NER. (a) In the absence of Rad26, the lesion is trapped in RNAPII and TC-NER is repressed. (b) At normal or moderately increased Rad26 activities, partial disruption of the interaction of Spt5 with RNAPII loosens the complex, which enables translesion transcription leading to exposure and repair of the DNA lesion behind the RNAPII complex. (c) At highly increased Rad26 activities, the binding of Spt5 to RNAPII is severely disrupted, leading to impairments of trans-lesion transcription and repression of TC-NER. Among multiple TC-NER repressors, only Spt5, which coordinates the repression, is indicated for clarity.

Rad26 appeared to be more active in evicting Spt5 from chromatin (Fig. 10). Still, we cannot rule out the possibility that a certain fraction of the overexpressed Rad26 is misfolded and not functional for TC-NER. It should be noted that, instead of facilitating TC-NER, enhanced transcriptional bypass of DNA lesions accomplished by Rpb1 mutations has been shown to actually attenuate TC-NER [44]. Therefore, Rad26 may facilitate TC-NER not just by promoting transcriptional bypass of UV photoproducts. Rad26 may also simultaneously promote the recruitment of NER factors by weakening the binding of Spt5 and other TC-NER repressors to RNAPII. This explains why Rad26 becomes completely or partially dispensable for TC-NER in the absence of TC-NER repressors [5]. However, it remains to be elucidated as to how NER proteins are recruited once the RNAPII moves past the lesion. Among all the known NER factors, only TFIIH appears to directly interact with RNAPII during transcription initiation. To date, there is no evidence that TFIIH directly interacts with RNAPII during transcription elongation (where TC-NER mainly occur). If a true transcription–repair coupling factor (i.e., a matchmaker between RNAPII and the NER machinery) exists in yeast remains to be determined.

A previous report showed that overexpression of Rad26 increased repair of CPDs in both the transcribed and nontranscribed strands of the *RPB2* gene, indicating that both TC-NER and GG-NER may be enhanced upon Rad26 overexpression [45]. However, we observed that TC-NER was unaffected when Rad26 was moderately overexpressed and attenuated when Rad26 was highly overexpressed. We also did not observe significant change of GG-NER upon moderate or high levels of Rad26 overexpression. The discrepancy between the previous report and our findings here might be due to the difference of Rad26 overexpression levels, which were not quantitatively measured in the previous study.

The promotion of transcriptional bypass of DNA lesions by Rad26 may be analogous to that of the human CSB, which has been shown *in vitro* to

promote the addition of one more nucleotide opposite the 3′ T of a TT CPD [32]. If CSB at a certain level of activity promotes transcription bypass of DNA lesions in human cells remains to be tested. Rad26 may also be analogous to the *Escherichia coli* Mfd in resolving stalling of an RNA polymerase at lesions by pushing the RNA polymerase forward [4,6,7]. However, unlike Rad26, which promotes transcriptional bypass of DNA lesions, Mfd displaces the polymerase from the template. Also unlike Rad26, which does not seem to directly recruit NER factors, Mfd has been shown to recruit the bacterial NER machinery by directly interacting with UvrA [4,6,7].

Materials and Methods

Yeast strains and plasmids

Yeast strains and plasmids used are listed in Supplemental Tables S1 and S2, respectively. Strains with their genomic genes tagged with three consecutive FLAG (3× FLAG) sequences were created by using PCR products amplified from plasmid p3FLAG-KanMX, as described previously [46].

Measurement of protein expression

Cells were cultured in synthetic minimal medium containing 2% lactate, 2% glycerol, and 2% ethanol (LGE) at 30 °C to late log phase (A600 ≈ 1.0). Galactose and $CuSO_4$ were added to the cultures to final concentrations of 2% and 1 mM, respectively. Aliquots were taken at different times of further incubation. Whole-cell protein extracts were prepared from the aliquots by using the procedure as described previously [47]. Proteins of interest were detected by Western blot with antibodies against the FLAG tag (M2, Sigma, for 3× FLAG tagged proteins), Rpb1 (8WG16, Biolegend; H14, Enzo Life Sciences), histone H3 (182,926, Abcam), GAPDH (184,193, Abcam), and Tubulin (GTX76511, GeneTex).

Assays of Rad26 ATPase activity

Cells expressing 3× FLAG-tagged wild-type and helicase motif mutant Rad26 from 25 ml of log phase culture were washed with and resupended in 0.5 ml of IP buffer [50 mM Tris–Cl (pH 7.4), 150 mM NaCl, 1 mM EDTA, 1 mM EGTA, 0.4 mM Na_4VO_3, 10 mM $Na_4P_2O_7$, 10 mM NaF, 0.5% NP-40, 1% Triton X-100, 0.1% SDS, 0.2 mM PMSF, and protease inhibitors]. After the addition of 0.5 ml of glass beads, the cells were lysed by 8 × 30-s pulses of bead beating. Cell debris was removed by centrifugation at 20,000*g* for 10 min at 4 °C. Fifteen micrograms of the anti-FLAG antibody was added to the lysate, and the mixture was incubated at 4 °C overnight with gentle rotation. Protein A-coated agarose beads (Sigma) were added to the mixture and incubated at 4 °C for 3 h with gentle rotation. After being washed twice with IP buffer containing 0.5 M of NaCl and twice with IP buffer, the beads were incubated with 0.5 μCi of [α-^{32}P]ATP in 20 μl of a reaction buffer [50 mM Tris–HCl (pH 8.0), 5 mM $MgCl_2$, 1 mM DTT, 0.1 mg/ml bovine serum albumin, 5% glycerol, 1 mg/ml of sonicated heat-denatured salmon sperm DNA] at 37 °C for 30 min. One microliter of the reaction was spotted onto a thin-layer chromatography (TLC) plate (Sorbent Technology) and air dried. The TLC plate was developed in 750 mM potassium phosphate (pH 3.5) and exposed to a phosphorimager screen.

Measurement of RNAPII and Spt5 associations with chromatin

Cells were cultured in LGE medium (see above) to late log phase. Galactose or $CuSO_4$ was added to the cultures to a final concentration of 2% or 1 mM to induce Rad26 or Rad26LM under the *GAL10* or *CUP1* promoter, respectively. After 4 h of further incubation for galactose-induced cells or 1 h of further incubation for $CuSO_4$-induced cells, the cultures were irradiated with 240 J/m^2 of 254 nm UV and incubated in YPG (1% yeast extract, 2% peptone, and 2% galactose) with or without 1 mM $CuSO_4$ at 30 °C. Aliquots of 30 ml were taken at different times of the incubation. For measuring association of RNAPII with chromatin, cells from the aliquots were directly pelleted. For measuring association of Spt5 with chromatin, cells from the aliquots were fixed with 1% formaldehyde for 30 min, quenched with 125 mM glycine, washed, and then pelleted. The cell pellet from each aliquot was mixed with 0.5 ml ice-cold cell lysis buffer [20 mM Hepes (pH 8.0), 60 mM KCl, 15 mM NaCl, 10 mM $MgCl_2$, 1 mM $CaCl_2$, 10 mM *N*-butyric acid, 0.8% Triton X-100, 0.25 M sucrose, 2.5 mM spermidine, 0.5 mM spermine, 2× concentrated protease inhibitor cocktail (P8125, Sigma-Aldrich), 1 mM PMSF, and 20 mM ribonucleoside-vanadyl complex (New England Biolabs)] and 0.5-ml acid washed beads. Cells were lysed by 8 × 30-s pulses of bead-beating. Residual intact cells (P1) were removed by centrifugation at 500*g* for 5 min (Supplemental Fig. S3A). The supernatant (S1) was centrifuged at 2000*g* for 20 min. The pellet (P2) was washed once with cell lysis buffer and twice with wash buffer [20 mM Hepes (pH 7.6), 450 mM NaCl, 7.5 mM $MgCl_2$, 10% glycerol, 1% NP-40, 0.5 M sucrose, 1 mM DTT, 0.125 mM PMSF, 2× concentrated of protease inhibitor, 20 mM ribonucleoside-vanadyl complex] (Supplemental Fig. S3A). To concentrate proteins from the supernatant fractions, an equal volume of phenol was added. After vortexing and centrifugation, the phenol phase was transferred to a

fresh tube. Proteins in the phenol phase were precipitated by mixing with 5 volumes of methanol containing 0.1 M of ammonium acetate and centrifugation at 16,000*g* for 30 min. The protein pellets were dissolved in SDS-PAGE gel loading buffer. To reverse formaldehyde crosslinks, the samples were boiled for 20 min. Rpb1, Spt5, histone H3, and GAPDH in the chromatin and supernatant fractions were analyzed by Western blot.

Repair analysis of UV-induced CPDs

Cells were cultured in LGE medium (see above) at 30 °C to late log phase, and galactose and $CuSO_4$ were added to the cultures to final concentrations of 2% and 1 mM, respectively. After 4 h of further incubation, the cultures of cells containing pGAL-RAD26 or pGAL-RAD26LM were harvested. After 1 h of further incubation, all other cultures were harvested. UV irradiation (120 J/m^2 of 254 nm UV), repair incubation and repair analyses of CPDs of the harvested cells were performed as described previously [44].

Analysis of transcription in the genomic GAL10 gene

Cells were grown in LGE medium (see above) to late log phase, and $CuSO_4$ was added to the cultures to a final concentration of 1 mM. After 1 h of further induction, the cells were irradiated with 240 J/m^2 of 254 nm UV. The irradiated and unirradiated cells were pelleted and resuspended in YPG medium containing 1 mM $CuSO_4$ and incubated at 30 °C. Aliquots were taken at different times of the incubation, and total RNA was isolated by using a hot acidic phenol method [48].

For Northern blot analysis, the total RNA was resolved on formaldehyde agarose gels and transferred onto Hybond-N^+ membranes (GE Healthcare) [49]. The *GAL10* transcripts were probed with a *GAL10* riboprobe *in vitro* transcribed from plasmid pGAL10b in the presence of [α-^{32}P] UTP (Supplemental Table S2) [49].

The procedure for creating a next-generation sequencing library of *GAL10* transcripts is outlined in Fig. 5. One picomoles of a biotinylated oligonucleotide (5′-ACTTTGTAACTGAGCTGTCATTTATATTGAAT-biotin) that is complementary to the 5′ end of the *GAL10* mRNA was mixed with 10 μg of total RNA in a volume of 100 μl. The mixture was heated at 95 °C for 10 min and 50 °C for 5 min. Ten microliters of streptavidin magnetic beads (Dynabeads M-280 streptavidin, Life Technologies) was mixed with the sample and incubated at room temperature for 30 min. The beads were sequentially washed with MBS [100 Mops, 1 M NaCl, and 5 mM EDTA (pH 8.0)], 0.1× MBS containing 0.5% SDS, 0.1× MBS, and H_2O. *GAL10* transcripts now attached to the beads were ligated to a 5′ phosphorylated and 3′ blocked adapter containing a UMI of 12 random nucleotides (Ns) (5′-phosphate-CCTGACNNNNNNNNNNNNAGATCGGAAGAGCGTCGTGT-inverted dT). The ligation was carried out in a 20-μl reaction containing 25 pmol of the UMI-containing adapter and 20 units of T4 RNA ligase (New England Biolabs) for 5 h at room temperature. The ligated *GAL10* transcripts were hybridized to a reverse transcription primer (5′-ACACGACGCTCT) by incubating the beads in 10 μl of 0.1× MBS containing 100 pm of the primer at 37 °C for 20 min. The beads were sequentially washed with 0.1× MBS containing 0.5% SDS, 0.1× MBS, and H_2O. The *GAL10* transcripts were then reverse transcribed into DNA fragments by incubating the beads in a 10-μl reaction containing 200 units of ProtoScript II reverse transcriptase (New England Biolabs) for 5 h at 42 °C. The reverse-transcribed DNA fragments were amplified by 20 cycles of PCR. Illumina-barcoded sequencing adapters were added to the amplified fragments by 8 cycles of PCR using primers containing the adapter sequences at the 5′ ends. The sequencing libraries prepared from different samples were combined, and the fragments with the insert sizes of no more than 800 bp were gel purified and sequenced 300 bp from both ends. We obtained a total of ~20 million reads for each of two biological repeats.

The sequencing reads from different samples were sorted based on their sequencing barcodes by using FASTQ/A Barcode Splitter and aligned to the *GAL10* gene sequence by using BWA-MEM. The sequencing errors were corrected, and PCR duplicates were removed based on the UMI sequences attached to the *GAL10* transcripts by sequentially using GroupReadsByUmi and CallMolecularConsensusReads (Fgbio, Fulcrumgenomics). The corrected reads were aligned to the *GAL10* gene sequence by using Bowtie2. The reads with a mapping quality of <30 were removed by using Samtools View. The number of transcripts with a specific length and 3′ nucleotide was counted and normalized to the total number of reads that are the same length or longer than the transcripts, and the length distribution and nucleotide(s) frequencies at the 3′ ends of the transcripts were obtained by using custom scripts. The numbers of nucleotide misincorporations in an internal site (i.e., not at the 3′ ends) of the *GAL10* transcripts were counted by using Pysamstats and normalized to the total number of reads across the site.

Statistical analyses

All experiments presented in this paper were repeated 1–3 times, depending on reproducibility and necessity. Student's *t* tests were used for statistical analyses.

Acknowledgments

This work was supported by NSF Grant MCB-1615550 from the National Science Foundation (to S.L.).

Conflict of Interest: The authors declare that they have no conflicts of interest with the contents of this article.

Appendix A. Supplementary data

Supplementary data to this article can be found online at https://doi.org/10.1016/j.jmb.2019.02.010.

Received 5 October 2018;
Received in revised form 12 January 2019;
Accepted 11 February 2019
Available online 18 February 2019

Keywords:
nucleotide excision repair;
RNA polymerase II;
Spt5;
Rad26;
UV photoproducts

Abbreviations used:
CPD, cyclobutane pyrimidine dimer; GG-NER, global genomic nucleotide excision repair; NER, nucleotide excision repair; RNAPII, RNA polymerase II; TC-NER, transcription coupled nucleotide excision repair; TLC, thin-layer chromatography; UV, ultraviolet.

References

[1] O.D. Scharer, Nucleotide excision repair in eukaryotes, Cold Spring Harb. Perspect. Biol. 5 (2013) a012609.
[2] D. Tatum, S. Li, Nucleotide excision repair in *S. cerevisiae*, in: F. Storici (Ed.), DNA Repair—On the Pathways to Fixing DNA Damage and Errors, InTech Open Access Publisher, Rijeka, Croatia 2011, pp. 97–122.
[3] E.L. Boetefuer, R.J. Lake, H.Y. Fan, Mechanistic insights into the regulation of transcription and transcription-coupled DNA repair by Cockayne syndrome protein B, Nucleic Acids Res. 46 (2018) 7471–7479.
[4] A.M. Deaconescu, M.M. Suhanovsky, From Mfd to TRCF and back again—a perspective on bacterial transcription-coupled nucleotide excision repair, Photochem. Photobiol. 93 (2017) 268–279.
[5] W. Li, S. Li, Facilitators and repressors of transcription-coupled DNA repair in *Saccharomyces cerevisiae*, Photochem. Photobiol. 93 (2017) 259–267.
[6] J.R. Portman, T.R. Strick, Transcription-coupled repair and complex biology, J. Mol. Biol. 430 (2018) 4496–4512.
[7] C.P. Selby, Mfd protein and transcription–repair coupling in *Escherichia coli*, Photochem. Photobiol. 93 (2017) 280–295.
[8] G. Spivak, Transcription-coupled repair: an update, Arch. Toxicol. 90 (2016) 2583–2594.
[9] W. Vermeulen, M. Fousteri, Mammalian transcription-coupled excision repair, Cold Spring Harb. Perspect. Biol. 5 (2013) a012625.
[10] P. Ruthemann, C. Balbo Pogliano, H. Naegeli, Global-genome nucleotide excision repair controlled by ubiquitin/Sumo modifiers, Front. Genet. 7 (2016) 68.
[11] L.C. Andrade-Lima, A. Veloso, M.T. Paulsen, C.F. Menck, M. Ljungman, DNA repair and recovery of RNA synthesis following exposure to ultraviolet light are delayed in long genes, Nucleic Acids Res. 43 (2015) 2744–2756.
[12] B.A. Donahue, S. Yin, J.S. Taylor, D. Reines, P.C. Hanawalt, Transcript cleavage by RNA polymerase II arrested by a cyclobutane pyrimidine dimer in the DNA template, Proc. Natl. Acad. Sci. U. S. A. 91 (1994) 8502–8506.
[13] C.P. Selby, R. Drapkin, D. Reinberg, A. Sancar, RNA polymerase II stalled at a thymine dimer: footprint and effect on excision repair, Nucleic Acids Res. 25 (1997) 787–793.
[14] S. Tornaletti, B.A. Donahue, D. Reines, P.C. Hanawalt, Nucleotide sequence context effect of a cyclobutane pyrimidine dimer upon RNA polymerase II transcription, J. Biol. Chem. 272 (1997) 31719–31724.
[15] F. Brueckner, U. Hennecke, T. Carell, P. Cramer, CPD damage recognition by transcribing RNA polymerase II, Science. 315 (2007) 859–862.
[16] J.S. Mei Kwei, I. Kuraoka, K. Horibata, M. Ubukata, E. Kobatake, S. Iwai, et al., Blockage of RNA polymerase II at a cyclobutane pyrimidine dimer and 6-4 photoproduct, Biochem. Biophys. Res. Commun. 320 (2004) 1133–1138.
[17] C. Walmacq, A.C. Cheung, M.L. Kireeva, L. Lubkowska, C. Ye, D. Gotte, et al., Mechanism of translesion transcription by RNA polymerase II and its role in cellular resistance to DNA damage, Mol. Cell 46 (2012) 18–29.
[18] S. Li, Transcription coupled nucleotide excision repair in the yeast *Saccharomyces cerevisiae*: the ambiguous role of Rad26, DNA Repair (Amst) 36 (2015) 43–48.
[19] S. Li, M.J. Smerdon, Rpb4 and Rpb9 mediate subpathways of transcription-coupled DNA repair in *Saccharomyces cerevisiae*, EMBO J. 21 (2002) 5921–5929.
[20] L.E. Jansen, H. den Dulk, R.M. Brouns, M. de Ruijter, J.A. Brandsma, J. Brouwer, Spt4 modulates Rad26 requirement in transcription-coupled nucleotide excision repair, EMBO J. 19 (2000) 6498–6507.
[21] B. Ding, D. LeJeune, S. Li, The C-terminal repeat domain of Spt5 plays an important role in suppression of Rad26-independent transcription coupled repair, J. Biol. Chem. 285 (2010) 5317–5326.
[22] W. Li, C. Giles, S. Li, Insights into how Spt5 functions in transcription elongation and repressing transcription coupled DNA repair, Nucleic Acids Res. 42 (2014) 7069–7083.
[23] D. Tatum, W. Li, M. Placer, S. Li, Diverse roles of RNA polymerase II-associated factor 1 complex in different subpathways of nucleotide excision repair, J. Biol. Chem. 286 (2011) 30304–30313.
[24] K.J. Armache, S. Mitterweger, A. Meinhart, P. Cramer, Structures of complete RNA polymerase II and its subcomplex, Rpb4/7, J. Biol. Chem. 280 (2005) 7131–7134.
[25] G.A. Hartzog, J. Fu, The Spt4-Spt5 complex: a multi-faceted regulator of transcription elongation, Biochim. Biophys. Acta 2013 (1829) 105–115.
[26] Y.Y. Chiou, J. Hu, A. Sancar, C.P. Selby, RNA polymerase II is released from the DNA template during transcription-

coupled repair in mammalian cells, J. Biol. Chem. 293 (2018) 2476–2486.
[27] D. Lejeune, X. Chen, C. Ruggiero, S. Berryhill, B. Ding, S. Li, Yeast Elc1 plays an important role in global genomic repair but not in transcription coupled repair, DNA Repair (Amst) 8 (2009) 40–50.
[28] L. Lommel, M.E. Bucheli, K.S. Sweder, Transcription-coupled repair in yeast is independent from ubiquitylation of RNA pol II: implications for Cockayne's syndrome, Proc. Natl. Acad. Sci. U. S. A. 97 (2000) 9088–9092.
[29] C. Mackinnon-Roy, L.J. Stubbert, B.C. McKay, RNA interference against transcription elongation factor SII does not support its role in transcription-coupled nucleotide excision repair, Mutat. Res. 706 (2011) 53–58.
[30] R.A. Verhage, J. Heyn, P. van de Putte, J. Brouwer, Transcription elongation factor S-II is not required for transcription-coupled repair in yeast, Mol. Gen. Genet. 254 (1997) 284–290.
[31] J. Xu, I. Lahiri, W. Wang, A. Wier, M.A. Cianfrocco, J. Chong, et al., Structural basis for the initiation of eukaryotic transcription-coupled DNA repair, Nature. 551 (2017) 653–657.
[32] C.P. Selby, A. Sancar, Cockayne syndrome group B protein enhances elongation by RNA polymerase II, Proc. Natl. Acad. Sci. U. S. A. 94 (1997) 11205–11209.
[33] J.P. Laine, J.M. Egly, Initiation of DNA repair mediated by a stalled RNA polymerase IIO, EMBO J. 25 (2006) 387–397.
[34] T. Borggrefe, R. Davis, A. Bareket-Samish, R.D. Kornberg, Quantitation of the RNA polymerase II transcription machinery in yeast, J. Biol. Chem. 276 (2001) 47150–47153.
[35] N.A. Kulak, G. Pichler, I. Paron, N. Nagaraj, M. Mann, Minimal, encapsulated proteomic-sample processing applied to copy-number estimation in eukaryotic cells, Nat. Methods 11 (2014) 319–324.
[36] L. Wang, O. Limbo, J. Fei, L. Chen, B. Kim, J. Luo, et al., Regulation of the Rhp26ERCC6/CSB chromatin remodeler by a novel conserved leucine latch motif, Proc. Natl. Acad. Sci. U. S. A. 111 (2014) 18566–18571.
[37] D. Lohr, P. Venkov, J. Zlatanova, Transcriptional regulation in the yeast GAL gene family: a complex genetic network, FASEB J. 9 (1995) 777–787.
[38] B. Ribar, L. Prakash, S. Prakash, Requirement of ELC1 for RNA polymerase II polyubiquitylation and degradation in response to DNA damage in *Saccharomyces cerevisiae*, Mol. Cell. Biol. 26 (2006) 3999–4005.
[39] T. Smith, A. Heger, I. Sudbery, UMI-tools: modeling sequencing errors in Unique Molecular Identifiers to improve quantification accuracy, Genome Res. 27 (2017) 491–499.
[40] D.E. Brash, S. Seetharam, K.H. Kraemer, M.M. Seidman, A. Bredberg, Photoproduct frequency is not the major determinant of UV base substitution hot spots or cold spots in human cells, Proc. Natl. Acad. Sci. U. S. A. 84 (1987) 3782–3786.
[41] L.A. Lindsey-Boltz, A. Sancar, RNA polymerase: the most specific damage recognition protein in cellular responses to DNA damage? Proc. Natl. Acad. Sci. U. S. A. 104 (2007) 13213–13214.
[42] S. Malik, P. Chaurasia, S. Lahudkar, G. Durairaj, A. Shukla, S.R. Bhaumik, Rad26p, a transcription-coupled repair factor, is recruited to the site of DNA lesion in an elongating RNA polymerase II-dependent manner in vivo, Nucleic Acids Res. 38 (2010) 1461–1477.
[43] B.S. Strauss, The “a” rule revisited: polymerases as determinants of mutational specificity, DNA Repair 1 (2002) 125–135.
[44] W. Li, K. Selvam, T. Ko, S. Li, Transcription bypass of DNA lesions enhances cell survival but attenuates transcription coupled DNA repair, Nucleic Acids Res. 42 (2014) 13242–13253.
[45] M. Bucheli, K. Sweder, In UV-irradiated *Saccharomyces cerevisiae*, overexpression of Swi2/Snf2 family member Rad26 increases transcription-coupled repair and repair of the non-transcribed strand, Mol. Microbiol. 52 (2004) 1653–1663.
[46] M.E. Gelbart, T. Rechsteiner, T.J. Richmond, T. Tsukiyama, Interactions of Isw2 chromatin remodeling complex with nucleosomal arrays: analyses using recombinant yeast histones and immobilized templates, Mol. Cell. Biol. 21 (2001) 2098–2106.
[47] V.V. Kushnirov, Rapid and reliable protein extraction from yeast, Yeast. 16 (2000) 857–860.
[48] M.A. Collart, S. Oliviero, Preparation of yeast RNA, in: F.M. Ausubel, R. Brent, R.E. Kingston, D.D. Moore, J.G. Seidman, J.A. Smith, et al., (Eds.), Current Protocols in Molecular Biology, John Wiley & Sons, Inc., New York, 2004 , (13.2.1-.2.5).
[49] J. Sambrook, D.W. Russell, Molecular Cloning: A Laboratory Manual, Cold Spring Harbor Laboratory Press, Cold Spring Harbor, NY, 2001.

Supplemental materials for "Evidence that moderate eviction of Spt5 and promotion of error-free transcriptional bypass by Rad26 facilitates transcription coupled nucleotide excision repair"

by Selvam et al.

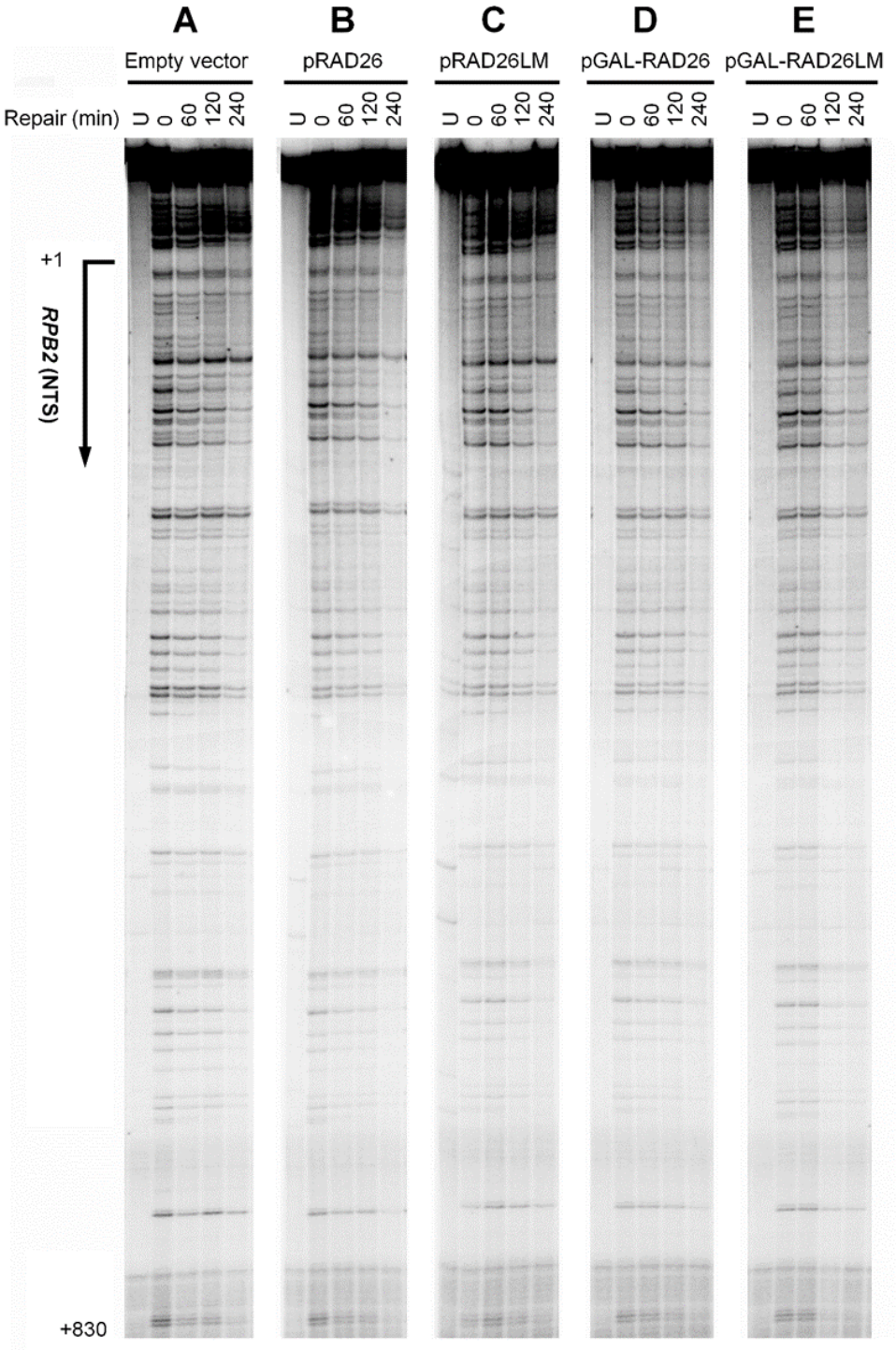

Supplemental Fig. S1. Repair of CPDs in the nontranscribed strand of the *RPB2* gene. *A-E*, sequencing gels showing CPDs remaining in galactose or $CuSO_4$ induced *rad26Δ* cells containing the indicated plasmids at different times of repair incubation. '*U*' indicates samples from unirradiated cells.

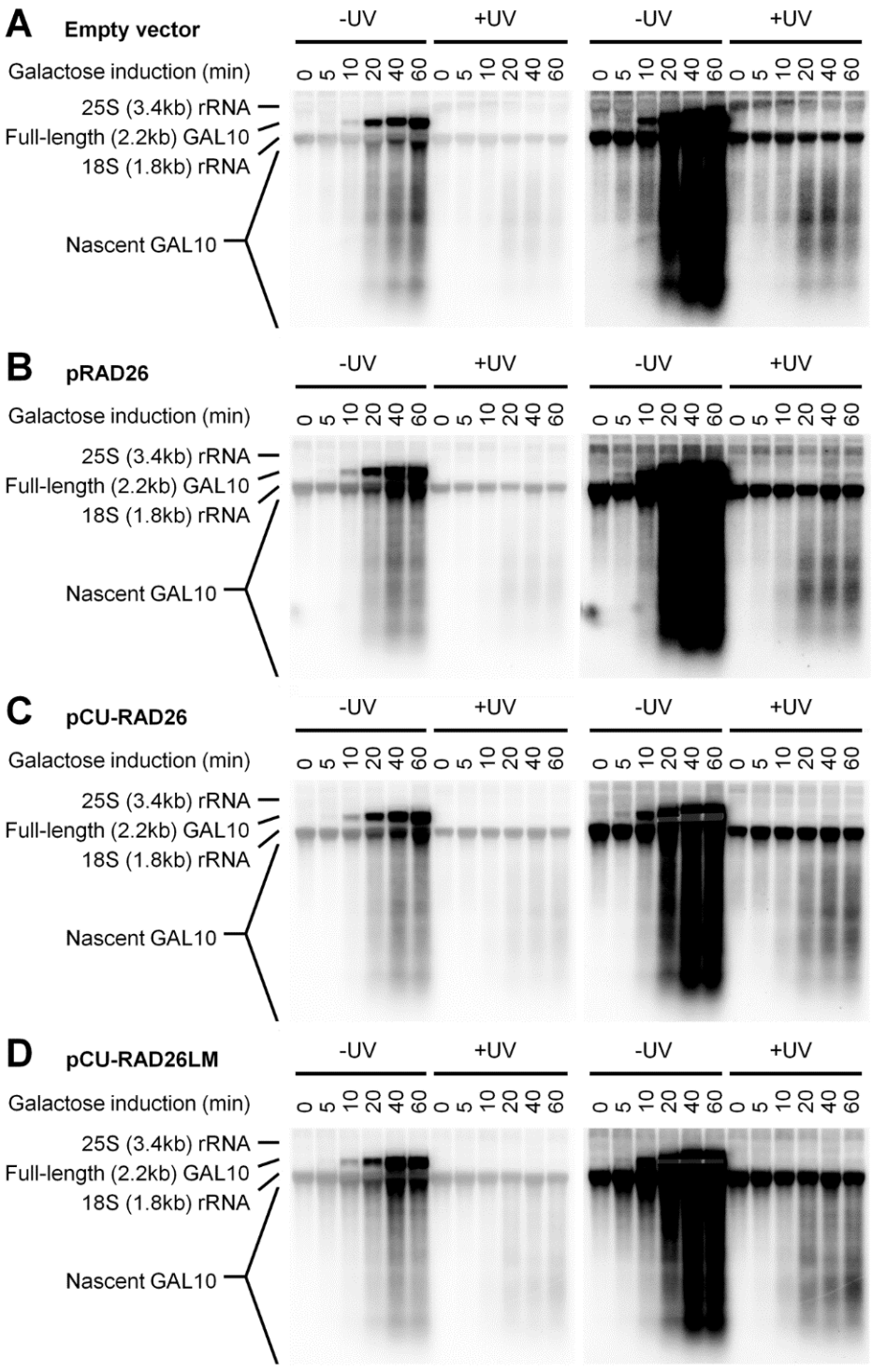

Supplemental Fig. S2. Galactose-induced transcription of the genomic *GAL10* gene. *A-D*, Northern blot showing *GAL10* transcripts in unirradiated and UV-irradiated *rad7Δ rad26Δ rad14Δ elc1Δ* cells containing the indicated plasmids at different times after galactose induction. The blots on the left and right are the same but with different exposures. The bands of abundant 25S and 18S rRNAs, which weakly cross hybridize to the *GAL10* probe, can be used as internal loading control.

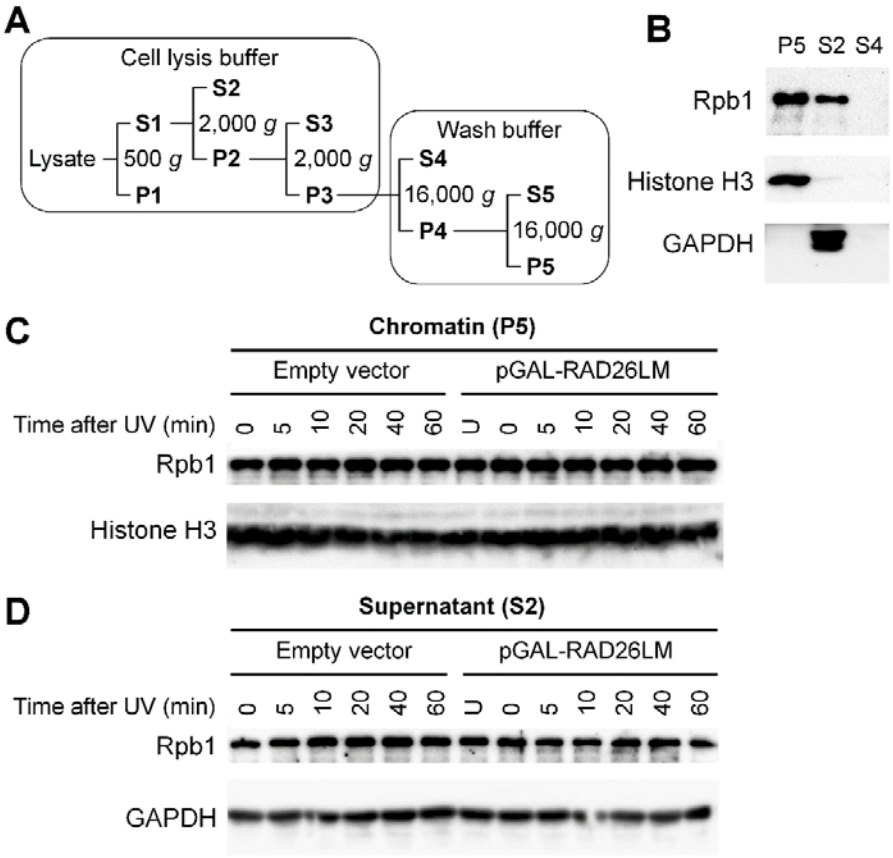

Supplemental Fig. S3. Distribution of Rpb1 (the largest subunit of RNAPII) between chromatin and nonchromatin fractions. *A*, scheme of the fractionation protocol. *B*, Western blots showing Rpb1, histone H3 and GAPDH in the different fractions prepared from unirradiated *rad7Δ rad26Δ rad14Δ elc1Δ* cells containing an empty vector. *C*, Western blots showing Rpb1 and histone H3 in the chromatin fractions prepared from *rad7Δ rad26Δ rad14Δ elc1Δ* cells containing the indicated plasmids at the indicated times after UV irradiation. *D*, Western blots showing Rpb1 and GAPDH in the supernatant fractions prepared from the same cultures as in (*C*). "U", sample prepared from unirradiated cells.

Supplemental Table S1. Yeast strains used.		
Strain	**Genotype**	**Ref./Source**
BJ5465	*MATa ura3-52 trp1 leu2Δ1 his3Δ200 pep4::HIS3 prb1Δ1.6R can1*	[1]
CR4	As BJ5465 but *rad7Δ rpb9Δ rad26Δ tfb5::URA3*	Lab stock
Y452	*MATα ura3-52 his3-1 leu2-3 leu2-112*	[2]
SL107	As BJ5465, but *rad7Δ*	Lab stock
CR46	*MATa ura3-52 pep4::HIS3 his3 leu2 rad7Δ rad26Δ* (derived from crossing between CR4 and Y452)	Lab stock
CR96	As SL107*, but* genomic *RPB2* tagged with 3×FLAG	Lab stock
KS696	As CR46, but *rad14Δ elc1::KanMX*	This study
KS1015	As SL107, but the genomic *RAD26* tagged with 3×FLAG	This study
WL588	As BJ5465, but *rad26Δ*	[3]

Supplemental Table S2. Plasmids used.		
Plasmid	**Description**	**Ref./Source**
pRS416 (empty vector)	Single-copy vector with *URA3* as election marker	[4]
pRAD26	A 4.5 kb sequence encompassing *RAD26* promoter, 3×FLAG tagged *RAD26* coding region and the *RAD26* terminator inserted between SacI and ClaI sites of pRS416	This study
pRAD26HIa	As pRAD26, but with *RAD26* codons K328A and T329C mutations	This study
pRAD26HVI	As pRAD26, but with *RAD26* codons Q759A and R763A mutations	This study
pRAD26HIa-VI	As pRAD26, but with *RAD26* codons K328A, T329C, Q759A and R763A mutations	This study
pRAD26-LM	As pRAD26, but with codons of leucines 18 and 21 of *RAD26* mutated to that of alanine	This study
pESC-URA	Multiple-copy vector with *URA3* as selection marker	Agilent
pGAL-RAD26	A 3.3 kb 3×FLAG tagged RAD26 sequence inserted between the *GAL10* promoter and *ADH1* terminator (SpeI and SacI sites) of pESC-URA	This study
pGAL-RAD26LM	As pGAL-RAD26, but with codons of leucines 18 and 21 of *RAD26* mutated to that of alanine	This study
pCU-RAD26	As pGAL-RAD26, but with the *GAL10* promoter replaced with the *CUP1* promoter	This study
p-CU-RAD26LM	As pGAL-RAD26LM, but with the *GAL10* promoter replaced with the *CUP1* promoter	This study
pGEM-3Z	Vector for cloning and in vitro transcription of sequences under SP6 and T7 RNA polymerase promoters	Promega
pGAL10-b	A 150 bp sequence immediately downstream of the transcription start site of the *GAL10* gene inserted between the EcoRI and SalI sites of pGEM-3Z	[5]

References:

[1] Jones EW. Tackling the protease problem in Saccharomyces cerevisiae. Methods Enzymol. 1991;194:428-53.
[2] Li S, Smerdon MJ. Rpb4 and Rpb9 mediate subpathways of transcription-coupled DNA repair in Saccharomyces cerevisiae. Embo J. 2002;21:5921-9.
[3] Li W, Selvam K, Rahman SA, Li S. Sen1, the yeast homolog of human senataxin, plays a more direct role than Rad26 in transcription coupled DNA repair. Nucleic Acids Res. 2016;44:6794-802.
[4] Sikorski RS, Hieter P. A system of shuttle vectors and yeast host strains designed for efficient manipulation of DNA in Saccharomyces cerevisiae. Genetics. 1989;122:19-27.
[5] Li W, Selvam K, Ko T, Li S. Transcription bypass of DNA lesions enhances cell survival but attenuates transcription coupled DNA repair. Nucleic Acids Res. 2014;42:13242-53.